

A data assimilative 1/12° North Atlantic hindcast experiment using HYCOM: towards a reduced Kalman filter approach

L. Parent (1), J.M. Brankart (2), O.M. Smedstad (3), A.J. Wallcraft (4), T.L. Townsend (4), P. Brasseur (2), H.E. Hurlburt (4), G.A. Jacobs (4) and E.P. Chassignet (5)

(1) Sverdrup Inc., Mississippi Office, MS 39525 e-mail: parent@nrlssc.navy.mil

phone number: (1) 228 688 5272 fax number: (1) 228 688 4759

(2) LEGI-CNRS, Grenoble, France

(3) Planning Systems Inc., Stennis Space Center, MS 39529

(4) Naval Research Laboratory, Stennis Space Center, MS 39529

(5) RSMAS/MPO, University of Miami, FL 33149

Short title: DATA ASSIMILATION

Abstract.

A $1/12^\circ$ North Atlantic hindcast experiment has been conducted by using the HYbrid Coordinate Ocean Model (HYCOM) and a data assimilation scheme derived from a reduced-order Kalman filter (the Singular Evolutive Extended Kalman filter, SEEK), whose main feature is that the analysis increment is obtained by the projection of the innovation vector (observations minus model counterparts) onto a limited number of Empirical orthogonal functions (Eofs), with the advantage of a large reduction computational requirements. This study extends some prior works to an eddy-resolving hindcast experiment at $1/12^\circ$ resolution for the period July 1998 - August 1999, with the assimilation of along track altimetry data, an operational sea surface temperature product and a sea surface salinity climatology every 7 days. In this paper, the global performance of this system is evaluated, first in term of RMS misfit or bias compared to the assimilated data, then to independent data (in-situ profiles). By comparison with a pure model simulation (no data assimilation), results show a significant improvement of the mean ocean state, with a correction of the bias, especially in the deep ocean (depths ≥ 500 meter). The positions and extensions of the fronts are much more realistic, due to the use of a relevant Mean Sea Surface Height (Mean SSH). The thermohaline structure deduced from this hindcast experiment verifies some assumptions and estimations of the meridional overturning cell and the northward heat transport.

Keywords: Ocean Model, Data Assimilation, Altimetry, Atlantic Ocean Circulation

1. Introduction

During the last decade, computational resources have increased in a dramatic way allowing simulations with very large computational requirements in the geophysical sciences. In 1996, the Japan Earth Simulator project initiated a long term challenge focused on global environment change problems, as part of the Global Change Prediction Plan (<http://www.es.jamstec.go.jp>). In this context, the development of an operational ocean system was estimated to be essential for society and human benefits. The international Global Ocean Data Assimilation Experiment project (GODAE, *International GODAE Steering Team*, [2000], <http://www.bom.gov.au/bmrc/ocean/GODAE>) emerged to establish the international collaborations necessary to meet the challenges of representing the oceans throughout the globe for analysis and prediction of the three-dimensional state of the ocean. After a few years, teams in different countries were constituted (Bluelink, ECCO, FOAM, HYCOM consortium, Japan-GODAE, MERCATOR, MERSEA, MFSPP, TOPAZ) to meet this goal as well as others. Even if sufficient computational power is available to run global ocean models, a system to provide ocean analysis and prediction must include additional components. The system must manage 3 main components: model, observation and assimilation technique. The realism of numerical ocean models has reached a level such that it is now possible to represent the observed ocean circulation with higher accuracy (*Smith and Maltrud*, [2000], *Chassignet and Garraffo*, [2001]). The observational network has become more highly developed: Sea Surface Temperature

(SST), Sea Level Anomaly (altimetry, SLA) and in-situ data (TAO (*McPhaden*, [1995]) and PIRATA (*Servain et al.*, [1998]) arrays, ARGO floats (*Argo*, [1998]), XBTs, multiple additional sources of moored and drifting buoy data, ...) are delivered in real-time. In addition, forcing fields are provided by atmospheric global circulation models (AGCMs). The challenge is to combine all this information in an optimal way through data assimilative ocean models. The background and the expertise gained from operational atmospheric systems is very helpful, and almost all current ocean data assimilation schemes are based on that experience. The goal of this study is to make a contribution or single step along the path to the long-term GODAE objective. This work is focused on the implementation of a reduced-order Kalman filter (Singular Evolutive Extended Kalman filter, SEEK, *Pham et al.*, [1998]) with a high-resolution ($1/12^\circ$) Atlantic configuration of the HYbrid Coordinate Ocean Model (HYCOM). This configuration is the ocean prototype system used to evaluate the performance before the transition to operational use by the U.S. Navy at the Naval Oceanographic Office (NAVOCEANO). In the fall of 2002, a near real-time data assimilation of SSH was put into place using Optimal Interpolation and the Cooper-Haines vertical projection (*Cooper and Haines*, [1996]) (<http://hycom.rsmas.miami.edu>). Some results of the current near real-time data assimilation are described in *Chassignet et al.* [2005]. Now, the HYCOM consortium is focussing on the implementation and evaluation of data assimilation techniques more sophisticated but with an affordable numerical cost. This work is based on earlier results from *Brankart et al.*, [2003] and *Birol et al.*, [2004], with a $1/3^\circ$ configuration of the MICOM or HYCOM ocean models. The results from their hindcast

experiments revealed that the system was not sufficiently accurate to be exploited by oceanographers or for operational use, but could constitute the backbone of an ocean system in return for some improvements. In this article, we describe the upgrade of this system by increasing the resolution of the model (from $1/3^\circ$ to $1/12^\circ$), which is very close to the resolution of along track altimetry data, with some improvements of the model source code and some minor modifications of the assimilation system. Note that the purpose of this paper is not a comparison of the results from a high and a low resolution configuration (it would be a subject of an other article), but mainly an estimation of the positive or adverse impacts of data assimilation with the use of a high resolution HYCOM configuration, and more specifically impacts on the mean state and its associated variability. That is intended as the main contribution of this article, even if a fully four dimensional description of a such an expensive ocean system needs much more effort and many more diagnostics. The paper is organised as follows. Section 2 presents an overview of this system, the primitive equation ocean model (HYCOM) used in the hindcast experiment, the SST, sea surface salinity (SSS) and SLA assimilated data as well as the Mean Sea Surface Height (Mean SSH), the assimilation scheme and the strategy. Section 3 describes the results considering two aspects, comparison with assimilated data and comparison with independent data (with a focus in 4 key areas: (1) Gulf Stream region, (2) Caribbean Sea and Gulf of Mexico, (3) Labrador Sea and (4) Irminger Sea, see figure 9). The global surface circulation is presented in section 4, as well as the zonally averaged transport and the mixed layer depth behavior. Finally, section 5 concludes on main insights of this hindcast experiment and the improvements

needed before transfer for operational use.

2. Numerical Model, datasets, assimilation system, strategy

2.1. Model Description and Configuration

The ocean model used is the HYbrid Coordinate Ocean Model (HYCOM) developed through the collaborative efforts of the University of Miami (RSMAS), the Naval Research Laboratory (NRL) and the Los Alamos National Laboratory (LANL).

The model configuration used here covers the North and Tropical Atlantic Ocean, including the Mediterranean Sea and spans from 98°W to 36°E and 28°S to 70°N . The Mercator grid has a longitude x latitude resolution of $0.08^{\circ} \times 0.08^{\circ} \cos\Theta$, where Θ is the latitude, and is referred to as a $1/12^{\circ}$ grid throughout the rest of the paper. It has 9 km resolution along the equator, 7 km around Cape Hatteras and 5 km in the Labrador Sea. A number of studies (*Hurlburt and Hogan*, [2000]; *Smith and Maltrud*, [2000]; *Maltrud and McClean*, [2005]; *Paiva et al.*, [2000]; *Chassignet and Garraffo*, [2001]) established that the horizontal grid spacing should be at least $1/10^{\circ}$ to resolve western boundary currents (e.g. Gulf Stream) and the mesoscale variability in a realistic way (the Rossby radius is around 20-40 km and less than 6 km north of 55°N). Moreover, a high resolution grid is necessary to resolve the baroclinic instability, which is an important physical process for deep convection events taking place, for example, in the Labrador Sea (*Marshall and Schott*, [1999]). With $1/12^{\circ}$ horizontal resolution, the configuration of the model is sufficient to be eddy-resolving and capable of representing ocean fronts

and the general pathway of the mean currents more realistic than an eddy-permitting resolution of $1/4^\circ$, *Smith and Maltrud*, [2000].

The main feature of HYCOM is the generalized vertical coordinate, which is a hybrid representation. It is isopycnal in the open stratified ocean and makes a dynamically smooth transition to a terrain-following coordinate (σ) in shallow coastal regions and fixed pressure-level coordinate (z) in the surface mixed layer and unstratified areas (*Bleck*, [2002]). Along the vertical axis there are 28 layers and the potential density is referenced to 20MPa ($\sim 2000\text{m}$), including the thermobaricity effect (*Sun et al.*, [1999]; *Chassignet et al.*, [2003]), which has a non-negligible impact on the HYCOM free sea surface height (SSH variable). The vertical mixing scheme used in this study is based on the K-Profile Parameterization model (*Large et al.*, [1994]). Other vertical mixing schemes are available in HYCOM (GISS, KT, MY, PWP), see *Halliwel*, [2004] for more details about the implementation, results and performances of the vertical mixing schemes. These choices have important effects on the representation of some characteristic waters masses such as the Antarctic Bottom Water (AABW) or the Mediterranean Outflow Water (MOW) in the Gulf of Cadix (*Chassignet et al.*, [2003]) and therefore can modify the overall circulation and the meridional overturning circulation (MOC).

The bottom topography is generated by using the Naval Research Laboratory Digital Bathymetry Data Base 2-minute resolution (NRL DBDB2) data set with hand-modifying in key regions such as straits or channels (Florida Straits, Lesser Antilles, ...), and slightly smoothed. The coastline is at the 5 meter isobath and the

minimum model depth is 10 meters. The simulations were initialized with the GDEM3 (Generalized Digital Environment Model version 3.0) climatology, a NAVOCEANO product (*Carnes*, [2003]). This monthly climatology is used to restore temperature, salinity and pressure interface in 3°-wide buffer zones adjacent to the closed northern and southern closed boundaries.

The model is spun up from rest during a 10-year time period with monthly climatological winds (wind stress, wind speed) from the ERA15 ECMWF reanalysis. Then, high-frequency (6 hourly) interannual anomalies from NOGAPS (Navy Operational Global Atmospheric Prediction System) / FNMOC (Fleet Numerical and Oceanography Center) wind fields are added to the ECMWF wind climatology to produce the interannual run. It started in July 1998, finished in September 2004 and the data-assimilative hindcast experiment is focused on the July 1998 - August 1999 time period. Bulk formulation (*Kara et al.*, [2002]) is used to estimate the heat fluxes from NOGAPS / FNMOC fields, the model SST and the above winds. There is no precipitation flux and the SSS is relaxed to the GDEM3 monthly climatology. Also, there is no SST relaxation in the reference experiment or in the experiment with assimilation.

2.2. Datasets

In the hindcast experiment, SSS, SST and altimetry data are assimilated (similar datasets as *Birol et al.*, [2004]).

2.2.1. SSS data. The SSS data come from the GDEM3 climatology. During the assimilation step, the ‘observed SSS’ is obtained by a linear time interpolation of two successive monthly values. The specified observation error is 0.05 psu. During the estimation of the innovation vector (observation minus model counterpart), there is a smoothing operator on the model SSS to take into account the very smooth climatology ($\sim 2^\circ$).

2.2.2. SST data. The SST data are from the MODAS (Modular Ocean Data Assimilation System) system (*Fox et al.*, [2002]) which is operational and runs daily at NAVOCEANO. This $1/8^\circ$ gridded SST product is based on a OI analysis of available MCSST observations and the specified observation error is 0.3°C . One disadvantage of this product is that it is probably too smooth in comparison to the resolution of the model ($1/12^\circ$, less than 10 km) or the resolution of original MCSST data (10 km), but a great advantage is that it covers the global ocean, which is not the case of MCSST data, especially in high latitudes and during the winter season (clouds). A smoothing operator is applied to the model SST prior to computing the innovation vector though the smoothing amplitude is less than for the SSS data.

2.2.3. Altimetry data. The altimetry data are delivered via NAVOCEANO’s Altimeter Data Fusion Center (ADFC). During the hindcast experiment (July 1998 - August 1999), only Topex/Poseidon and ERS-2 along track data are available. For a 7 day time window, there are around 100,000 along track altimetry observations in the domain. The specified observation error is 3 cm. Details of the altimeter data processing may be found in *Jacobs et al.*, [2001a]. Before the use of altimetry data there is a crude

quality control (sensitivity check). If the absolute value of the altimetry signal is beyond 5 standard deviations, the data are rejected. Moreover, if the absolute value of the altimetry signal deviates more than 1.5 meters, the data are not used.

Finally, due to the uncertainty of the tidal model on the shelves and the fact that the satellite altimetry is not able to give accurate data nearer than 14 kms from the coasts, a mask is applied so that the altimetric observations are not used along the model coastline and on the shelves.

We do not use any SST, SSS or SSH observation located in the buffer zones. That is to avoid the estimation of an innovation vector with a large and unrealistic amplitude during the analysis stage, which can cause strong non-physical corrections and bad model response in or close to the boundaries.

2.2.4. Mean SSH data. To assimilate the altimetry signal, a Mean Sea Surface Height (Mean SSH) is required. *Birol et al.*, [2004] and *Crosnier and LeProvost*, [2005] showed that the results of data assimilation can be changed in a dramatic way by the choice of a Mean SSH and the estimation of a Mean SSH is a priority issue for operational oceanography, since it can introduce a systematic bias. The selected Mean SSH has to satisfy different properties :

- 1 The mean must represent the large scale ocean dynamics in a correct manner with e.g. a realistic balance between subpolar and subtropical gyres or between open ocean and semi-enclosed seas (Mediterranean Sea, Gulf of Mexico).

- 2 It must contain an accurate position and extension of the frontal structures (Gulf Stream, Loop Current, Azores Current, ...).
- 3 There must exist narrow and intense flow (strong and realistic gradient) in key areas as Florida Strait or Yucatan Channel to represent a realistic mass transport.
- 4 The mean must be consistent with the model dynamics. In practice, this means that the observed Mean SSH must have the same reference level as the model Mean SSH or that the model drift (because of an incorrect flux balance or numerical issues) has to be much smaller than the mean difference between the observed Mean SSH and the model Mean SSH.

There are several Mean SSH products from which to choose. For a large part, Mean SSH products come from model simulations with or without some objective or subjective modifications (*Smedstad et al.*, [2003]; *Chassignet et al.* [2005]), from inverse model of the ocean circulation (*Legrand et al.*, [2003]), to the estimation of the dynamic height of an ocean climatology or built from different sources of data (*Rio and Hernandez*, [2004]; *Niiler et al.*, [2003]). *Lunde et al.*, [2005] made a comprehensive comparison of different Mean SSH products and showed that the Niiler Mean SSH (*Niiler et al.*, [2003]) is the best observation based Mean SSH in the North Atlantic area. The resolution of this Mean SSH product is $1/2^\circ$, covers the world ocean and has been estimated over the 1992-2002 period. One shortcoming is that some areas are missing in the Tropical band, along a part of the coastal areas of Africa, some shelf areas and the Mediterranean Sea. The Niiler Mean SSH was therefore remapped to the HYCOM grid and some additional processing was performed. The gaps in the Mean SSH field were filled either by spatial

interpolation or by merging with the Mean SSH used by *Chassignet et al.*, [2005].

Finally, we checked the remapped product and decided to mask areas where there was an obvious problem (it might come from the original Mean SSH (e.g. Florida Strait) or the processing), or where the assimilation of altimetry is not reliable (Gibraltar Strait, ...).

Figure 1 shows the Mean SSH product used for the assimilation of altimetry. The large scale structure is very realistic with a good balance between the subtropical and the subpolar gyres. A good reason to use this Mean SSH product is the position of the Gulf Stream and its connection with the Azores Current, which is not easily achievable in a model simulation (*Chassignet and Garraffo*, [2001]; *Özgökmen et al.*, [2001]). The black line of figure 1 represents the mean axis of the Gulf Stream determined from T/P data (*Lee*, [1997]). There is a high correlation between this mean axis and the position of the Gulf Stream from the Niiler Mean SSH (approximately represented by the zero contour line). The subpolar gyre exhibits 2 branches (Labrador Sea, Irminger Sea) with a small southward extension east of Newfoundland and the Grand Banks, and the quasi-permanent Mann Eddy (44°W, 42°N) is clearly visible. The geostrophic current deduced from this Mean SSH (figure 4 of *Niiler et al.*, [2003]) shows a realistic circulation from the Gulf Stream area to the extension of the North Atlantic Drift (NAD). The flow turns north of the Mann Eddy from 42°N to 52°N approximately, then turns eastward at about 51°N to form the NAD and its associated meanders. The Loop Current in the Gulf of Mexico also has a realistic pathway and has a strong signature.

The shape of the Mean SSH near the connection between the subtropical gyre

and the tropical band (40-60°W, 5-15°N) does not look very realistic. In this area, the North Brazil Current (NBC) follows the South American coast, then a part of this current retroflects to form the North Equatorial Countercurrent (NECC) whereas the other part encounters the south branch of the subtropical gyre circulation (North Equatorial Current, NEC) before it enters to the Caribbean Sea. The isolines of the Niiler Mean SSH are close to being parallel with latitudes in the southern part of the subtropical gyre, whereas in the reference simulation, or the Rio Mean SSH (*Rio and Hernandez, [2004]*), there is an angle of about 30-45° with latitudes. This results in a less intense flow from the NEC to the Caribbean Sea. The end result is that the assimilation experiment presents a large decrease in the intensity of the NECC in the retroreflection area and there is a much more connection between the NBC and the flow in the Caribbean Sea (see section 4.1 and figure 11). Note that this area is not the focus of this work, and this needs to be further investigated.

2.3. Assimilation System

The assimilation scheme is based on a reduced-order Kalman filter and is derived from the SEEK filter. This sequential method uses a representation of the error covariance matrix in a vector basis of small dimension, which limits the rank of the error covariance matrix (a key issue with such expensive configuration of the model). It has been used and validated in a number of studies (*Brankart et al., [2003]*; *Birol et al., [2004]*) and the reader can refer to these references for more details about the characteristics, the implementation and the physical adjustment operator needed

because of the particular vertical coordinate of HYCOM. Here, we briefly describe the minor modifications to the system.

In a classical way, the initial error covariance matrix is estimated with an Eof analysis of the model variability. The Eof analysis has been performed using model outputs over the period 1998-2001 from the model simulation without assimilation (reference run). The time interval between successive archive files used in the Eof analysis is 14 days. An error covariance matrix based on the first 8 Eofs is used to perform the assimilation experiment. After initial attempts, it was found that the crude use of these Eofs was not well suited with this eddy-resolving configuration. The analysis state was noisy, due to an inconsistency between the shape of the Eofs (small scale) and the shape of the innovation vector (a mix of large scale and mesoscale structures). To resolve this problem, we applied a smoothing operator to each archive file before the Eof analysis. Figure 2 shows the effect of the smoothing operator. Figure 2 a and b show the spatial distribution of the Eof 4 (SSH component) for a low resolution ($1/3^\circ$) and for the high resolution ($1/12^\circ$) configuration without smoothing. The impact of the mesoscale dynamics is clearly seen in the high resolution configuration. Structures are smaller and the signal has a higher amplitude than in the low resolution configuration (note that the $1/3^\circ$ configuration is eddy-permitting). Figure 2 c and d show the results of the Eof analysis when a smoothing operator is applied with a medium effect (18 x 18 points, $\sim 1.15^\circ$ at 40°N) or with a large effect (36 x 36 points, $\sim 2.3^\circ$ at 40°N). We decided to use the smoothing operator with a large effect (36 x 36 points) to perform the hindcast experiment. It allows a more stable solution in comparison with the medium effect

of the smoothing operator and numerical issues are greatly reduced. Note, that this approach needs further investigation in order to estimate and validate the correct length scale and it should be done by comparison of the ocean dynamics, RMS misfit, bias and model response between the low and high resolution configurations of the ocean model.

Another way to consider this issue is to look at the analysis stage of the SEEK filter. Each correction is the result of a linear combination of the Eofs and the weight applied to each Eof is proportional to the projection of the innovation vector on the Eof. There are different options to make the correction, depending on the goal of the assimilation, i.e a better representation of the interannual variability or the seasonal cycle, a reduction of the bias or a better control of the mesoscale activity. In this paper, our aim is to reduce the bias, see figure 7 for an estimation of the SST bias, and to control the mesoscale activity.

In order to do so, a local gain operator is introduced where each water column is only influenced by observations in a predetermined area. In parallel, it excludes long-range correlations which are not reliable or significant for the mesoscale and could bring spurious influence through large-scale signatures in the Eofs (e.g. from the North Sea to the Gulf of Mexico). If the influence radius is very small (it means that the water column is influenced by few observations), there is a strong projection of the local innovation vector on the Eof in the predetermined area, and implied a large local correction, but the global analysis state could present a noisy signature. On the other hand, if the influence radius is too large, there is a weak or no correction and the analysis state is similar to the forecast state. So the challenge is to determine a good

combination between the length of the influence radius, the spatial pattern of the Eofs (means applying a strong, weak or no smoothing operator) and the spatial pattern of the innovation vector. In practice, after the choice of the amplitude of the smoothing operator, we found that an influence radius of 700 km allowed the assimilation analysis to produce a stable model solution.

The last modification, which is more of a pragmatic issue than a ‘pure theoretical assimilation consideration’, is to apply a reduced correction in sensitive areas. Figure 3 represents the factor by which the correction is multiplied. It limits large modifications of the ocean state in regions where the accuracy of the altimetry data is low, where the assimilation is not practical (e.g. Bahamas straits) or where the numerical stability of the ocean model is delicate.

2.4. Strategy

The 1/12° North Atlantic configuration is very expensive in terms of computer time, memory and human time. The dimensions of the grid are 1678 x 1609 x 28 (~76 million points) of which about 46% are ocean points. Over land points, no calculations are performed and no computer memory is used. The size of an archive file is 2.3Gb and 40K cpu hours are needed to run a one year simulation without assimilation (IBM 1.3GHz POWER4). It means that a 7 days simulation takes 2.4 elapsed hours with 320 processors. Because of this numerical cost, it was not possible to produce more than a one year experiment or different assimilation experiments to define the best set of parameters. Note that the simulation without data assimilation (reference experiment)

is not the latest run. The HYCOM team conducts some tests to reduce the shortcomings of this simulation, e.g. by tuning the values of the tracer and momentum diffusivities. In the next sections, we will describe results (quantitative and qualitative aspects) of our hindcast simulation during the July 1998 - August 1999 period. We consider that a one year hindcast experiment is the minimum length time needed to evaluate such an assimilation experiment.

Here is the summary of the experiment.

The assimilation frequency is 7 days and the analysis stage is performed each Wednesday. The first analysis stage is July, 8th 1998 and the last one is August, 4th 1999. The assimilated data are T/P and ERS-2 along track data, MODAS SST and GDEM3 SSS. The relaxation to SSS climatology is the same as in the reference experiment and there is no SST relaxation. The only model difference between the reference and assimilation experiments is that the Bottom Boundary Layer (BBL) parameterization is turned on in the assimilation experiment, as it allows a better representation of the Mediterranean Outflow Water.

Unless explicitly noted, all diagnostics are performed with the 7 day forecast state rather than the analysis state, and the time mean of any variable is computed over the period August, 5th 1998 - August, 4th 1999. The first month (July 1998) is not used because there are strong adjustments during the first analysis stages. We will not describe the data management of this assimilation experiment, as it is beyond the scope of this paper, but it is an important component of the success of such experiment.

3. Hindcast experiment : July 1998 - August 1999

3.1. Comparison with SSH, SST data : RMS misfit and bias

The first test is to evaluate the performance of the assimilation system by comparing the results with the assimilated data. Figure 4 represents the RMS misfit with respect to the T/P along track data (left panel) and MODAS SST (right panel) (see figure 9 to locate the diagnostic areas). The general behavior is classical. During the first assimilation steps there is a strong reduction in the RMS misfit (mainly the bias), then the amplitude of the misfit is stable and follows the reference experiment in parallel. The red and black crosses along the vertical axis represent the bias between the observations and the model counterparts. For the SST data, the estimation of the mean difference is computed between the 7-day forecast and observed SST from August 1998 to August 1999 (53 archive files). For the SSH data, it is more complicated because along track data are used. We assume that a correct estimation of the bias can be done by computing the difference between the model Mean SSH (August, 5th 1998 to August, 4th 1999, based on 7-day forecast states) and the Niiler Mean SSH (it is probably more correct if the time period is longer). The amplitude of the bias is not negligible for the SSH data as well as for the SST data. It represents 70% of the SSH misfit over the Atlantic model domain and around 60% for the Gulf Stream region. For the SST, it represents 70 to 80 % or more in particular areas. The assimilation of SSH and SST data reduces a large part of the bias, especially in the Gulf Stream area.

To identify the origin of the discontinuity between the 7-day forecast and the

previous analysis state, the RMS misfit with the MODAS gridded altimetry product was estimated (dashed black and blue curves of the left panels of figure 4). This gridded product is based on an OI analysis of T/P and ERS2 along track data with covariances estimated by *Jacobs et al.*, [2001b]. The MODAS system uses a large data window (in space and time) and tends to smooth a large part of the mesoscale signal contained in the along track observations. In addition, the RMS misfit between the along track T/P data and the gridded MODAS data was estimated for the 1998-1999 period (see figure 5). To perform this, the gridded data are projected along T/P fixed track positions and the RMS misfit is calculated for each T/P cycle (~ 10 days). The difference reveals that the RMS misfit between gridded data and along track data is around 6 cm for the Atlantic model domain and 10 cm for the Gulf Stream region.

The RMS misfit of the experiments compared to gridded altimetry data presents a general reduction of the amplitude in comparison with the RMS misfit to along track T/P data, from 2-3 cm in the Atlantic model domain to 4-7 cm in the Gulf Stream area. The behavior is more steady and there are much smaller differences between the 7-day forecast state and the previous analysis state. This demonstrates that a large part of the discontinuity is not due to an incorrect analysis state (non-physical or not consistent with the model constraints), but it is mainly due to the mesoscale dynamics. For future simulations, this issue has to be better understood and probably resolved by some improvements in the estimation of the error covariance matrix (to split large scale and mesoscale dynamics).

The magenta curve represents the RMS misfit with respect to the observations

when the assimilation is turned off for the last 2 months of the simulation. The behavior of the SSH and SST variables is very different. There is a small increase of the overall SSH RMS misfit during the first month, after which the RMS misfit asymptotes. Nevertheless, after 2 months, the Gulf Stream tends to overshoot and a small ring appears near the Cape Hatteras (but much smaller than in the reference simulation). The large drift in the Caribbean Sea is linked to the formation of a Loop Current eddy. In the assimilation experiment, the Loop Current is clearly visible (August, 4th 1999, last archive file available) and the northwestern part of the Loop Current is thinner but the eddy is not yet detached. After 2 months without assimilation, the eddy is not in agreement with observations and is present in the middle of the Gulf of Mexico whereas the Loop Current is confined to the southern part of the Gulf of Mexico and with a much smaller extension. It demonstrates that the formation, the extension, the amplitude and the pathway of such eddies are non-deterministic and it need to be continuously controlled by data assimilation.

More problematic is the SST drift when the assimilation is turned off. Remember that the model is forced only by bulk formula using atmospheric fields and model SST, there is no SST relaxation to any SST product (see section 2.1). After 2 months, the RMS misfit has the same amplitude as the reference simulation (Atlantic model domain), although it is lower in some areas (Gulf Stream) and higher in others (Mediterranean Sea). Careful examination of the results showed that there is a large scale bias in SST in response to heat fluxes (black and red crosses of figure 4 ; see figure 7 for an estimate of the bias) and represents the main part of the misfit. Each assimilation step tends to

correct the SST bias, but the 1-day forecast presents a large discontinuity in comparison with the analysis state. Then, during the following 6-day of the forecast, the differences between 2 successive daily model SST are weaker and weaker. One of the underlying assumptions of the assimilation system is that the model, forcing and observation errors are Gaussian distributed random variables with a priori characteristics. If this assumption were true, the mean correction during the August, 5th 1998 to August, 4th 1999 period should correspond to the a priori characteristics and so exhibits a white noise (see figure 6). For the SSH variable, it is mainly true, except along the pathways of the Gulf Stream, the North Atlantic Current (NAC) and the Loop Current. For the SST variable, it is not the case as it should be. There is a large SST correction in the Gulf Stream area and the Subtropical gyre. There appears to be an imbalance between the assimilated MODAS SST data, the thermal fluxes (shortwave, longwave radiations) and the model interpretation of the surface fluxes. Some sections across the domain revealed that surface layers from the reference simulations are colder than observations. Figure 7 shows the bias between the model SST and MODAS SST observed. The bias exhibits a marked dipole along the observed Gulf Stream pathway (more than 2.5°C). The main reason is that the reference simulation has an overshoot with a permanent ring close to Cape Hatteras. The ring tends to bring warm waters too far north along the US and Canadian coastlines whereas it is too cold south of the observed Gulf Stream. Another characteristic of the SST bias is its scale and amplitude. For a large part of the domain, the model SST is too cold, especially in the subtropical gyre. In the northern part, the model is too warm close to the coasts of Greenland and Canada, along the

Labrador, Eastern and Western Greenland Currents. With the assimilation of MODAS SST, the bias is reduced almost everywhere. The large cold bias disappears as well as the warm bias north of the Gulf Stream. East of Iceland, the warm bias is reduced and it reveals a more realistic Norwegian Current (see figure 11). A small part of the bias is still present, along the coastline and close to or in the buffer zones. One reason is that the assimilation system is mainly dedicated to the control of the deep ocean dynamics (depths ≥ 500 meters), and a mask is applied to limit the correction in the shallow areas and the buffer zones (see figure 3). Another reason is that in the Labrador or Irminger Seas, sea ice is present along a large part of the coastline. This version of the model has only an energy loan ice model (and not a dynamic-thermodynamic sea ice model) and the current assimilation scheme does not include the sea ice variable.

For future simulations, it will be important to obtain better control of the SST bias by improving the model surface forcing, rather than using sequential SST corrections. Correction of the bias in the longwave / shortwave fluxes could be done before the use of these forcing fields (preprocessing, see *Large and Yeager, [2004]*), or by turning on the SST relaxation. A more sophisticated solution is to include forcing fields in the state vector and to apply a correction determined by the data assimilation. Note that the variational approach to data assimilation is better adapted to tackle this issue (*Stammer et al., [2004]*).

The last conclusion regarding the diagnostics in figure 4 is that even if SSH and SST RMS misfits present similar behaviors (bold black and red curves), the discontinuity between the 7-day forecast and the previous analysis stage does not represent the same

kind of error sources. For the SSH variable, it is mainly due to a lack of control of the mesoscale dynamics while for the SST variable it is due to a lack of control of the large scale bias.

3.2. SSH variability

Figure 8 represents the standard deviation (STD) of SSH variability during the hindcast experiments in comparison to the MODAS altimetry product (during the August, 5th 1998 - August, 4th 1999 period). As mentioned earlier, the MODAS SSH gridded data are smooth compared to the original along track data. That is the main reason why the STD has a larger amplitude in the reference or assimilation experiments than the MODAS gridded SSH fields. Close to the coast, on the shelves and at high latitude the MODAS system excludes data and underestimates the variability. The reference experiment (middle panel) has a spurious eddy close to Cape Hatteras and too much variability south of the observed Gulf Stream pathway (60-75°N). While observations show that the Mid-Atlantic ridge acts as a wall for the propagation of the SSH variability toward the east, the reference simulation exhibits a continuous pattern of high variability from Cape Hatteras to Ireland. The behavior of the assimilation experiment is closer to the MODAS variability and more realistic. The permanent ring is no longer present, the variability decreases east of the Mid-Atlantic ridge and the Azores Current variability is better estimated. In the Gulf Stream area, the SSH variability of the assimilation experiment seems to be located too far south compared to independent observations (solid black lines). This may be due to interannual variability, and thus a

longer hindcast experiment is needed to verify this. From the Venezuela coast to the Gulf of Mexico, the variability of the reference simulation is much stronger than the MODAS observations. In the Caribbean Sea, it could be due to the propagation of too many eddies compared to observations. In the Gulf of Mexico, it is due to the movement of an eddy, when there was no observed eddy during this time period. This may be a consequence of the ~ 1 year analysis, which is insufficient to remove statistical anomalies such as single Loop Current eddies. The assimilation produces a better estimate of the variability in the Caribbean Sea and Gulf of Mexico. Along the Greenland coast, the assimilation decreases the variability. Perhaps the Eastern and Western Greenland Currents are more stable, but inside the Irminger and Labrador Seas, the variability is slightly stronger.

3.3. Comparison with independent temperature data

3.3.1. GDEM3 climatology. The correct way to evaluate the impact of the assimilation is to compare to data which have not been used during the assimilation experiment. In our case this is in-situ data. The disadvantage is that the in-situ data are sparse in time and in space compared to surface data. First, the GDEM3 climatology can be used to compare the general mean behavior. Figure 10 represents the RMS misfit between the annual mean climatology and the annual mean ocean state from the reference and assimilation experiments. To perform this diagnostic, a vertical remapping along fixed depths was applied and only profiles where the depth is greater than 500 meters are used. The analysis is conducted in 4 different regions (Gulf Stream

region, Caribbean Sea and Gulf of Mexico, Labrador area, and Irminger area, see figure 9). In all selected regions the data assimilation gives a reduction in the RMS misfit from climatology, especially in the upper 600 meters. The most noticeable improvement is found in the Gulf Stream region, where the mean pathway of the current is more realistic. This has a strong impact on the vertical structure. Even in the sensitive Labrador and Irminger areas, there is an improvement along the vertical direction. A large part of the improved estimate of the vertical temperature structure is due to the use of the Niiler Mean SSH, which is a good product in many areas. At the surface, the reduction of the RMS misfit is due to the assimilation of the MODAS SST combined with the GDEM3 SSS. It allows warmer temperature in the surface layers and decreases the model bias. The main residual error is located between 50 and 150 meters, where the seasonal thermocline is positioned. In this depth range, a difference of a few dozens of meters in the vertical position of the water masses between observation and model is sufficient to create this misfit. The control of the thermocline is probably the present great challenge of data assimilation in an operational oceanography context. The assimilation of in-situ data could improve the representation of the seasonal thermocline (see *Birol et al.*, [2004]), and will be included in future experiments.

3.3.2. MEDS in-situ profiles. The validation with in-situ MEDS (Marine Environmental Data Services, <http://www.meds-sdmm.dfo-mpo.gc.ca>) data shows the same behavior (figure 10). To perform this comparison, MEDS data and model counterparts are interpolated onto a common vertical and horizontal grid. Then the in-situ temperature is estimated from potential temperature and salinity model

variables and only profiles where the depth is more than 500 meters are used. The RMS misfit is larger compared to MEDS profiles than to the GDEM3 climatology, but the improvement due to the data assimilation is larger close to the seasonal thermocline position (50-100 meters) in the Gulf Stream and Irminger regions. The vertical discontinuity around the seasonal thermocline is not as sharp (i.e, smoother) when compared to the MEDS data than to the GDEM3 climatology. On the whole, the mean vertical temperature structure of the assimilation experiment is closer to the GDEM3 climatology or in-situ MEDS profiles than the reference experiment. Nevertheless, with this diagnostic, the vertical impact of the assimilation of surface data on the mesoscale dynamics cannot be estimated.

4. The Atlantic domain circulation

4.1. The surface circulation

Here, the mean surface circulation over the Atlantic model domain will be described as well as the improvements or adverse effects introduced by the assimilation. The description is split in 2 parts (see figure 11). The first part is focused on the south west circulation from the North Brazil Current (NBC) to the Gulf Stream and the second part describes the circulation from the North Atlantic Current to the subpolar gyre.

4.1.1. Southwest circulation. Along the South American coast, the NBC has a large intensity and the retroflexion is located at about 8°N . In parallel, the NEC current feeds the Caribbean Sea. Data assimilation, through the use of the Niiler Mean

SSH, changes these dynamics in a large way. The retroreflection area is located farther south with a reduced intensity. The Caribbean Sea seems to receive the main flow from the NBC rather than the NEC. From the Lesser Antilles to the Yucatan Channel, the flow does not show much change. The assimilation experiment exhibits a more narrow Caribbean Current which tends to be located farther south and closer to the South American coast. South of Cuba, there is a more intense eastward current which comes from a small anticyclonic recirculation of the Caribbean Current. Regarding the southward (inward) surface flow through the Windward Passage (between the islands of Cuba and Hispanola), the assimilation tends to reduce the intensity of this flow, which is not realistic (see figure 14 of *Johns et al.*, [2002] for a schematic representation of the circulation in the Caribbean Sea). The Loop Current has the same shape with a small increase in intensity, as well as the westward coastal current along the Louisiana and Texas coastlines. In the western part of the Gulf of Mexico, the reference simulation has a large Loop Current eddy, which is not observed during this time period. The assimilation removes this eddy and the Yucatan current (about 95°W - 23°N) is present between the southern cyclonic (95°W - 20°N) and the northern anticyclonic (95°W - 25°N) pair. Then, the Loop Current feeds the Florida Current through the Florida Straits. The assimilation experiment exhibits a less intense Florida Current. It is probably due to the use of a low resolution ($1/2^{\circ}$) Mean SSH compared to the resolution of this model configuration ($1/12^{\circ}$). Another change is that the Antilles Current, located just north of the Greater Antilles islands, is less intense and it seems to receive a larger part of the flow through the Bahamas straits in the assimilation experiment. Note that the

southeast flow through the Old Bahamas Channel (between the Bahamas and Cuba) is not realistic. It should be northwest and the assimilation does not improve this coastal circulation.

East of the Cape Hatteras, the reference simulation presents an unrealistic permanent anticyclone. This particular feature is well known in the ocean modeling community. It reveals that the resolution is not the only necessary parameter to produce a realistic western boundary current (see the difference in the Gulf Stream pathway in a global $1/10^\circ$ ocean simulation of the POP model, *Maltrud and McClean*, [2005] and the $1/10^\circ$ North Atlantic configuration of the POP model, *Smith and Maltrud*, [2000], or the impact of the viscosity parameterization on the Gulf Stream separation with MICOM (*Chassignet and Garraffo*, [2001])). The assimilation experiment exhibits a much more realistic pathway of the Gulf Stream, from Cape Hatteras to the Mann Eddy (44°W , 42°N), even though there is still a weak northward flow along the US coast (Mid-Atlantic Bight).

4.1.2. Northeast circulation. The Gulf Stream splits into 2 parts around the position of the Mann Eddy. South of 38°N , the assimilation experiment has the Azores Current which flows southward and then eastward (at about 34°N), whereas the reference experiment is not able to produce this southern branch. North of the Mann Eddy, the NAC is more clearly visible in the assimilation experiment. The North Atlantic Drift (NAD) and its associated meanders spread into a large part of the north eastern domain. The data assimilation allows a more intense northward flow, toward the subpolar gyre (limited by the 4000 m topographic contour). Then it turns east and

the meanders are less and less intense from 37°W to 10°W. In the reference simulation, the mean flow in the north eastern part of the domain has the same structures, with a lot of meanders, but much stronger and not as realistic. The reference run exhibits some permanent anticyclones (25°W-55°N, 23°W-53°N, 23°W-58°N) close to a topographic slope (2000 m topographic contour). Note that thanks to a new set of values of the tracer and momentum diffusivities, results seems better in the latest non-assimilative simulation.

East of the Iceland / Faroe axis, the Norwegian Current has a better pathway in the assimilation experiment (see plate 6 of *Fratantoni*, [2001] and figure 7 of *Poulain et al.*, [1996] for a schematic representation of the surface currents). A part of the flow comes from the inflow of Atlantic water thanks to the NAD through the Iceland basin and the Rockall trough, whereas the other part comes from a cyclonic circulation in the Norwegian basin. The reference simulation has a strong eastward flow from the Atlantic while the Iceland / Faroe flow is not clearly visible. With the assimilation, the Iceland / Faroe flow is clearly seen and the Norwegian Current follows the 2000 meter topographic contour. It allows a stronger SST gradient across the Iceland / Faroe axis and is more consistent with observations (WOCE drifters, see figure 2 of *Treguier et al.*, [2005]). North of 65°N, the mean circulation cannot be evaluated because this region lies within the buffer zone.

In the subpolar gyre circulation, modifications are not as large. The Irminger Current follows the 2000 m topographic contour, then merges with the Eastern Greenland Current, turns north after Cape Farewell to form the Western Greenland

Current. It then turns west and then south to feed the Labrador Current through 2 branches (61°N and 63°N) and it is in reasonable agreement with results obtained by *Cuny et al.*, [2002]. But the 61°N branch from the assimilation experiment is probably too intense and the Western Greenland Current disappears north of 63°N. The southward penetration of the Labrador Current (close to 47-50°W, from 50°N to 43°N) through the Flemish Pass basin (west of the Flemish Cap) is more intense in the assimilation experiment (see the barotropic signal, figure 12). It is closer to the results obtained by *Smith and Maltrud*, [2000] and is more consistent with observations (WOCE drifters, see figure 2 of *Treguier et al.*, [2005]). It allows a stronger southward flow of cold surface water and a larger SST gradient between this flow and the warm water from the Gulf Stream. Then, the Labrador Current meets the Gulf Stream and retroflects. In the reference simulation, a large part of the flow of the Labrador Current turns east, north of the Flemish Cap, which is less realistic. An adverse effect of the assimilation is that the SST in the area south of the Flemish Cap / Flemish Pass basin is too cold whereas it is too warm in the reference simulation (see figure 7 in the vicinity of 47°W-44°N).

4.1.3. Atlantic circulation - summary. The assimilation experiment produces a stronger gradient of the barotropic streamfunction between the subtropical and the subpolar gyres (see figure 12), which is more realistic in comparison with other assimilation experiments performed with other ocean models (*Crosnier and LeProvost*, [2005]). Nevertheless, the maximum of the barotropic streamfunction is reduced from 29.4 to 27.1 Sv at 27°N in the Florida Strait (the position of the STACS cable, where

the observed mean transport is estimated to be around 30-33 Sv, *Baringer and Larsen, [2001]*) as a result of a too smooth Mean SSH. Note that it is not the case with the use of a high resolution model Mean SSH (see *Chassignet et al. [2005]*).

In conclusion, the circulation in the assimilation experiment is much more realistic than the reference simulation, except east of the Lesser Antilles or close to the Greater Antilles. The impact of the assimilation has some adverse effects on the shelf break areas or close to the coast. Even with the use of a limited correction mask (see figure 3), the flow through some key straits or passages is modified. However, in some places the reference simulation exhibits currents that are spurious or too intense close to the shelf break. For example, there is an intense unobserved westward current south of Iceland which follows the Reykjanes Ridge, and another one located at 63°W - 62°N , a problem that needs further investigation.

4.2. The overturning circulation and the meridional heat transport

Integral diagnostics for the mean ocean dynamics have been computed from the reference and assimilation experiments. In the case of a simulation without assimilation (reference experiment), the time evolution of the three-dimensional ocean dynamics is continuous and there are no artificial sources or sinks. With a sequential data assimilation, this is no longer true. The variational approach of data assimilation (*Stammer et al., [2004]*), which is able to produce a time smooth solution of the ocean dynamics, seems to be better suited to deal with such diagnostics, but that is less true when the configuration of the ocean model uses a high resolution grid ($1/12^{\circ}$). The

reason is that the approximation of the tangent linear model is valid only for a short time period and that implies the need to reduce the length of the assimilation cycle. That creates some discontinuities after each assimilation cycle, as in our sequential data assimilation approach. In addition, the ocean model has to deal with the results of the analysis stage and the imbalanced fluxes, so it can generate a conflict if we look at some global physical diagnostics.

The meridional overturning circulation is shown in figure 13. The overturning represents the overall vertical structure from the southern to the northern boundaries and has a classical behavior. The meridional overturning cell is driven by the thermohaline circulation. The overflows of dense water through the Denmark and Iceland Straits and the convection in the Labrador Sea create the North Atlantic Deep Water (NADW) which covers the mid-depth ocean and spreads toward the south as a deep western boundary current. It is balanced by a northward flow of warm surface water advected by the western boundary current (Gulf Stream). In the reference simulation, the maximum overturning is 17 Sv at 25°N at about 1000 m depth, and the overturning cell (≥ 12 Sv) has a very thin and has a small meridional extension. It is not possible to directly observe the overturning circulation and its amplitude, but a consensus tends to estimate the maximum value from 17 to 21 Sv. *Hall and Bryden*, [1982] estimates the strength of the MOC to 19.33 Sv at 25°N. A near global 1/10° MOM simulation (*Masumoto et al.*, [2004]), with an unrealistic position of the Gulf Stream and NAD, estimate the maximum value at 17.4 Sv. From the global 1/10° POP simulation (*Maltrud and McClean*, [2005]), the value is about 23 Sv whereas the North

Atlantic $1/10^\circ$ POP simulation estimates the maximum to 23.9 Sv (*Smith and Maltrud, [2000]*). Note that in this latest case, the Gulf Stream and NAD pathways are realistic. The reference experiment tends to underestimate the overturning circulation and the assimilation increases the overturning cell in a significant way. The maximum is 25.5 Sv at the same location but 100 m deeper. The meridional extent of the overturning cell (≥ 12 Sv) is much broader and covers nearly the whole domain. Results from the assimilation experiment are more consistent with results from other ocean models, especially the meridional extent, but it tends to overestimate the maximum by 3-5 Sv as well as the vertical extent. Note that this result is very sensitive to the choice of the northern and southern boundaries, the choice of the vertical coordinate in HYCOM and even more to the assimilated Mean SSH.

The local minimum shown at 30°N , 400 m depth is due to a small recirculation structure east of the Florida Current. An adverse effect of the assimilation is that the extent of the AABW is too small (depths ≥ 3500 m, streamfunction ≤ 0 Sv) and confined to the southern hemisphere. This water mass is slightly better represented in the reference simulation but is too weak in comparison with results of *Chassignet et al., [2003]*.

Figure 14 shows the mean meridional heat transport of the reference and the assimilation experiments. To calculate the mean meridional heat transport, we use 53 archive files of the assimilation experiment (7-day forecast). Unfortunately, for technical reasons, this diagnostic is available with only 10 archive files, unevenly spaced out of the reference experiment. So the comparison could be biased or not well defined.

Moreover, this estimate is obtained by using instantaneous ocean states of a high resolution model. *Crosnier et al.*, [2001] and *Jayne and Tokmakian*, [1997] established that at such a resolution, the estimation of some diagnostics are biased because of inertial oscillations. Aliasing errors can be as large as 0.2 PW in the tropics and the behavior is much more noisy in the tropical band ($\pm 15^\circ$) (see figure 3 of *Crosnier et al.*, [2001]). To fix this problem, it turned out that the time average over a 5 day period is sufficient to limit the aliasing effect. The mean heat transport estimated from these instantaneous ocean states exhibits a noisy signal all along the latitude band (thin curves of figure 14). To bypass this issue and to present a more convenient diagnostic, we smoothed the instantaneous ocean states with a 6° latitude window and estimate the standard deviation from these smoothed snapshots (thick dashed curves, done only for the assimilation experiment).

Comparisons with estimations from *Ganachaud and Wunsch*, [2003] and *McDonald and Wunsch*, [1996] are consistent in the northern hemisphere. The maximum of the mean heat transport from the assimilation experiment is around 1.32 PW in the 20-30°N latitude band and decreases toward the north. The mean heat transport of the reference experiment is around 0.9 PW in this latitude band (crude approximation). *Böning et al.*, [1996] established that there is a linear relationship between the maximum overturning and the heat transport close to 25°N (with an increase of 0.1 PW for every 2 Sv increase in the meridional overturning). Here, even if there are some issues about the aliasing effect, the number of snapshots available from the reference simulation and approximations, this linear relationship is still valid. The assimilation allows an increase

of 8.5 Sv (from 17 to 25.5 Sv) of the maximum meridional overturning cell whereas the heat transport increases from 0.9 PW to 1.27 PW in the 20-30°N latitude band (an increase of 0.37 PW). In our case, the increase is about 0.09 PW for every 2 Sv increase in the meridional overturning. In the equatorial band this diagnostic is not reliable, especially the shape of the curves. The presence of local maxima is an unrealistic feature of a mean estimate (it should be a smooth increase along the equatorial band, see *Crosnier et al.*, [2001]) and it is due to the aliasing effect.

4.3. The mixed layer depth and the salinity bias

The mixed layer depth in the northern part of the domain is shown in figure 15 (top panel, time average throughout the month of March 1999) as well as the SSS bias (bottom panel, time average throughout the period August, 5th 1998 - August, 4th 1999). In this region, the mixed layer depth reaches its maximum annual value in March and the deep convection phenomenon occurs mainly in the Labrador Sea. The NAO (North Atlantic Oscillation) index is about 2.0 for the period January - March 1999, which means that the deep convection is normal but not as intense as during the beginning of the nineties. The reference simulation exhibits an unrealistic pathway: the mixed layer has a similar depth and extension in the Labrador and Irminger Seas and there is a narrow deep mixed layer all along the Iceland / Greenland / Canada shelf break. The convection in the Irminger basin can occur but is not as large as in the Labrador Sea (the maximum mixed layer depth is supposed to be located in the vicinity of the bravo station, 51.5°W, 56.5°N). It is still unclear why the mixed layer depth is so

deep, close to the shelf break. It might be due to the advection of too much salty water mass due to the Irminger Current and the Eastern / Western Greenland Currents. The annual mean SSS bias (figure 15, bottom panel), is very large and can reach 0.8 psu close to Cape Farewell and Cape Desolation. It means that the SSS relaxation is not a good way to control the surface salinity close to the coast and in high latitudes, where the presence of ice increases the uncertainty, especially as there is no precipitation flux. The assimilation can improve the SSS and mixed layer depth behavior. The time evolution of the RMS misfit compared to the GDEM3 SSS climatology is displayed on figure 16. The largest improvement occurred during the fall and winter in the Labrador area. The amplitude of the SSS bias is reduced in the assimilation experiment by a factor of 2 to 3 times in the deep ocean of the Labrador Sea and there is a considerable improvement close to the coastline (see figure 15). This occurs even with the use of a limited correction mask (see figure 3). Between Iceland and Greenland, a large bias is still present but it is located in or close to the northern boundary. Along the vertical axis (see figure 17), the RMS misfit to the GDEM3 salinity is large and the assimilation experiment is much closer to the climatology, even though there is a small adverse effect below 250 meters depth in the Labrador area. The general improvement of the mixed layer depth seems to be due to a global surface water mass change in this area and not due to modifications of the circulation (which are weak in comparison with other areas). The Irminger Current feeds the area above the Reykjanes Ridge with warmer water, the assimilation of SST and SSS data allows a strong reduction of the SST and SSS bias along the Greenland coast, and the amplitude of the SSS relaxation is smaller

in the assimilation experiment. Thanks to the recirculation inside the Labrador and the Irminger Seas, it can change the vertical structure (temperature and salinity) and induce a more realistic mixed layer depth. The adverse effect of the assimilation is that the local maximum of the mixed layer depth in the Labrador Sea is probably too deep (≥ 2000 meter, grey color, in the vicinity of 48°W , 59°N), as well as the local maximum northeast of the Outer Hebrides islands (about 10°W , 58°N). Note that the flow in the assimilation experiment through the Iceland basin and the Rockall trough is less intense (see figure 11) and with less variability (see figure 8) than in the reference experiment, which can generate a deeper mixed layer west of the Iceland / Faroe axis.

5. Discussion and Conclusion

In this work, an assimilation scheme, derived from the SEEK filter, has been used to assimilate along track altimetry (from the T/P and ERS2 altimeters), an operational SST product (MODAS) and SSS climatology (GDEM3) to produce a hindcast experiment with a high resolution ($1/12^\circ$) configuration of the HYCOM model in the North Atlantic over the period July 1998 - August 1999. We have demonstrated that this system (model, data and assimilation scheme) is able to produce a realistic three-dimensional ocean state and dynamics for this time period. The bias has been reduced in a dramatic way and the mean flow is much more consistent with the observed ocean state and previous realistic ocean model simulations at such resolution (*Smith and Maltrud*, [2000]; *McCLean et al.*, [2002]; *Chassignet and Garraffo*, [2001]). In comparison with results obtained from an eddy-permitting configuration of HYCOM ($1/3^\circ$, *Birol*

et al., [2004]), the increase in the resolution allows a better propagation of the surface data into the three-dimensional thermohaline structure and improved and more realistic surface ocean dynamics (currents). This is due also to the use of a realistic MSSH product. The focus of this work is on the main positive and adverse effects of data assimilation in a high resolution configuration of HYCOM thanks to a large, objective and expensive validation. The goal was not a comparison of the results from the high and low resolution configurations or to estimate by data assimilation the impact of higher resolution in HYCOM. That should be an interesting subject but in a different paper.

Nevertheless, before transfer of this work to operational use, some issues still remain:

- A high resolution realistic and consistent Mean SSH is required to produce correct and useful output from an ocean operational data assimilation system (GODAE goal).
- HYCOM needs some improvements to obtain a better mean behavior without data assimilation. Some problems are linked to numerical schemes or parameterization of physical processes (numerical stability, spurious currents and deep mixed layer depth along the shelf break), others to the thermohaline state (choice of the initial state, SSS / SST relaxation, forcing fields). The HYCOM team conducts some tests to reduce the shortcomings of this reference experiment, e.g. by tuning the values of the tracer and momentum diffusivities, the mixed layer model or modifications of the bottom topography. Results of the most recent simulation seems better and more realistic.
- The assimilation system (model, data, assimilation scheme) has some problems in

the Mediterranean Sea and in the tropical band (not shown here). The origin of the problem in the Mediterranean Sea is still unclear. Regarding the tropical band (where the assimilation is turned off), it is due to a different ocean dynamics. The assimilation approach used in this paper (local correction) has not been optimized for this area, where the aim of the data assimilation is mainly to control the bias, the seasonal or interannual signal, but not the mesoscale dynamics (long-range correlation, see *Parent et al.*, [2003]).

- In the mid or high latitudes, the system needs to better control the mesoscale dynamics and to limit discontinuities after each analysis step. The Incremental Analysis Update (IAU, *Bloom et al.*, [1996]; *Ourmières et al.*, [2004]) could be considered.

- Along the vertical axis, the assimilation of vertical T/S profiles in addition to surface data will be able to limit the bias located around the seasonal thermocline (see *Birol et al.*, [2004]).

- SST data have to be better assimilated and be more consistent with heat fluxes.

Instead of using the operational MODAS SST product (which is too smooth in comparison with the resolution of the model), an other way could be to assimilate not one but two datasets :

+ a low resolution product with an error of 2-3°C (e.g. Reynolds SST).

+ a high resolution product with an error of 0.3°C (e.g. AVHRR data).

With this dual SST product, one can expect to control large area where no high resolution data are available (clouds) without deteriorating results in areas cover by high resolution data, but the tuning is very sensitive.

Note that a new SST product (GHRSSST, Global ocean data assimilation experiment High-Resolution Sea Surface Temperature), will be soon available and could improve results of data assimilation.

- Last, but not the easiest issue is to develop an assimilation system which is able to control the ocean dynamics close to the coast and on the shelf, and be dynamically consistent with the deep ocean assimilation system. It is still unclear what could be the right strategy. Some research is under way to deal with the small number of useful observations (no reliable along track altimetry data or Mean SSH, for example) and that can implies major modifications due to the coastal / shelf ocean dynamics and its control by the wind forcing.

Acknowledgments. This work was sponsored by the National Ocean Partnership Program (NOPP) and the Office of Naval Research (ONR) through the following projects: HYCOM Consortium for Data-Assimilative Ocean Modeling and U.S. GODAE: Global Ocean Prediction with the HYbrid Coordinate Ocean Model (HYCOM). Results were obtained under a FY04-08 Department of Defense (DoD) HPC Challenge and non-Challenge Projects, using the IBM SP4 at the Naval Oceanographic Office, Stennis Space Center, MS.

References

- Argo Science Team (1998), On the design and implementation of Argo: An initial plan for a global array of profiling floats, *International CLIVAR Project Office Rep. 21, GODAE Rep. 5, GODAE Project Office, Melbourne, Australia*, 32 pp.
- Baringer, M.O. and J.C. Larsen (2001), Sixteen years of Florida Current transport at 27°N, *Geophysical Research Letters*, *28*, 16, 2001GL013246, 3179–3182.
- Birol, F., J.M. Brankart., F. Castruccio, P. Brasseur and J. Verron (2004), Impact of the ocean mean dynamic topography on satellite data assimilation, *Marine Geodesy*, *27*, 59–78.
- Bleck, R. (2002), An oceanic general circulation model framed in hybrid isopycnic-cartesian coordinates, *Ocean Modelling*, *4*, 55–88.
- Bloom, S.C., L.L. Takacs., A.M. da Silva and D. Ledvina (1996), Data assimilation using incremental analysis updates, *Monthly Weather Review*, *124*, 6, 1256–1271.
- Böning, C.W., F.O. Bryan, W.R. Holland and R. Döscher (1996), Deep-water formation and meridional overturning in a high-resolution model of the North Atlantic, *Journal of Physical Oceanography*, *26*, 1142–1164.
- Brankart, J.M., C.E. Testut, P. Brasseur and J. Verron (2003), Implementation of a multivariate data assimilation scheme for isopycnic coordinate ocean models: Application to a 1993-1996 hindcast of the North Atlantic Ocean circulation, *Journal of Geophysical Research*, *108*, 10.1029/2001JC001198.
- Carnes, M.R. (2003), Description and Evaluation of GDEM-V 3.0, *Naval Oceanographic Office Technical Note*, 28 pp.
- Chassignet, E.P, H.E. Hurlburt, O.M. Smedstad, G.R. Halliwell, P.J. Hogan, A.J. Wallcraft,

- R. Baraille and R. Bleck (2003), The HYCOM (HYbrid Coordinate Ocean Model) Data Assimilative System, *Journal of Marine Systems*, accepted.
- Chassignet, E.P., L.T. Smith, G.R. Halliwell and R. Bleck (2003), North Atlantic simulations with the hybrid coordinate ocean model (HYCOM): Impact of the vertical coordinate choice, reference pressure, and thermobaricity, *Journal of Physical Oceanography*, *33*, 2504–2526.
- Chassignet, E.P. and Z.D. Garraffo (2001), Viscosity parameterization and the Gulf Stream separation, In *"/From Stirring to Mixing in a Stratified Ocean"/*. *Proceedings 'Aha Huliko'a Hawaiian Winter Workshop. U. of Hawaii. January 15-19, 2001. P. Muller and D. Henderson, Eds.*, 37–41.
- Cooper, M. and K. Haines (1996), Altimetric assimilation with water property conservation, *Journal of Geophysical Research*, *101*, 1059–1078.
- Crosnier, L. and C. Le Provost (2005), Inter-Comparing Five Forecast Operational Systems in the North Atlantic and Mediterranean basins : The MERSEA-Strand1 Methodology, *submitted to Journal of Marine Systems*.
- Crosnier, L., B. Barnier and A.M. Treguier (2001), Aliasing inertial oscillations in a $1/6^\circ$ Atlantic circulation model: impact on the mean meridional heat transport, *Ocean Modelling*, *3*, 21–31.
- Cuny, J., P.B. Rhines, P.P. Niiler and S. Bacon (2002), Labrador Sea boundary currents and the fate of the Irminger Sea Water, *Journal of Physical Oceanography*, *32*, 627–647.
- Fox, D.N., W.J. Teague, C.N. Barron, M.R. Carnes and C.M. Lee (2002), The modular ocean

- data assimilation system (MODAS), *Journal of Atmospheric and Oceanic Technology*, *19*, 240–252.
- Fratantoni, D.M. (2001), North Atlantic surface circulation during the 1990's observed with satellite tracked drifters, *Journal of Geophysical Research*, *106*, 22067–22093.
- Ganachaud, A. and C. Wunsch (2003), Large-Scale Ocean Heat and Freshwater Transports during the World Ocean Circulation Experiment, *Journal of Climate*, *16*, 696–705.
- Hall, M.M. and H.L. Bryden (1982), Direct estimates and mechanisms of ocean heat transport, *Deep Sea Research*, *29*, 339–359.
- Halliwel, G.R. (2004), Evaluation of vertical coordinate and vertical mixing algorithms in the hybrid coordinate ocean model (HYCOM), *Ocean Modelling*, *7*, 285–322.
- Hurlburt, H.E and P.J. Hogan (2000), Impact of $1/8^\circ$ to $1/64^\circ$ resolution on Gulf Stream model-data comparisons in basin-scale subtropical Atlantic ocean models, *Dynamics of Atmospheres and Oceans*, *32*, 283–329.
- International GODAE Steering Team (2000), Global Ocean Data Assimilation Experiment Strategic Plan, available at <http://www.bom.gov.au/bmrc/ocean/GODAE>, *GODAE Report No6*, 36 pp.
- Jacobs, G.A, C.N. Barron, D.N. Fox, K.R. Whitmer, S. Klingenberg, D. May and J.P. Blaha (2001a), Operational Altimeter Sea Level Products, *Oceanography*, *15*, 13–21.
- Jacobs, G.A, C.N. Barron and R.C. Rhodes (2001b), Mesoscale Characteristics, *Journal of Geophysical Research*, *106*, C9, 19581–19595.
- Jayne, S.R. and R. Tokmakian (1997), Forcing and sampling of ocean general circulation

- models: impact of high-frequency motions, *Journal of Physical Oceanography*, *27*, 1173–1179.
- Johns, W.E., T.L. Townsend, D.M. Fratantoni and W.D. Wilson (2002), On the Atlantic inflow to the Caribbean Sea, *Deep Sea Research Part 1*, *vol 49*, 211–243.
- Kara, A.B., P.A. Rochford and H.E. Hurlburt (2002), Air-Sea Flux Estimates and the 1997-1998 ENSO Event, *Boundary-Layer Meteorology*, *103*, 439–458.
- Large, W.G. and S.G. Yeager (2004), Diurnal to decadal global forcing for ocean and sea-ice models: the data sets and flux climatologies, *NCAR Technical Note NCAR/TN-460+STR*, 111 pp.
- Large, W.G., J.C. Mc Williams and S.C. Doney (1994), Oceanic vertical mixing: a review and a model with a nonlocal boundary layer parameterization, *Reviews of Geophysics*, *32*, 363–404.
- Lee, H. (1997), A Gulf Stream Synthetic Geoid for the TOPEX altimeter, *M.S. Thesis, Rutgers University. New Brunswick, New Jersey*, 36 pp.
- LeGrand, P., E.J.O. Schrama and J. Tournadre (2003), An inverse modelling estimate of the dynamic topography of the ocean, *Geophysical Research Letters*, *30*, *2*, 1062, 2002GL014917.
- Lunde, B.N., O.M. Smedstad, E.P. Chassignet and H.E. Hurlburt (2005), Comparing mean dynamic topography with in-situ estimates, *in preparation*.
- Maltrud, M.E. and J.L. McClean (2005), An eddy resolving global $1/10^\circ$ ocean simulation, *Ocean Modelling*, *8*, 31–54.

- Marshall, J. and F. Schott (1999), Open-ocean convection: Observations, theory, and models, *Reviews of Geophysics*, *37*, 1–64.
- Masumoto, Y., H. Sasaki, T. Kagimoto, N. Komori, A. Ishida, Y. Sasai, T. Miyama, T. Motoi, H. Mitsudera, K. Takahashi, H. Sakuma and T. Yamagata (2004), A fifty-year eddy-resolving simulation of the world ocean, preliminary outcomes of OFES (OGCM for the Earth Simulator), *Journal of the Earth Simulator, Volume 1, April 2004*, 35–56.
- McClean, J.L., P-M. Poulain, J.W. Pelton and M.E. Maltrud (2002), Eulerian and Lagrangian statistics from surface drifters and a high-resolution POP simulation in the North Atlantic, *Journal of Physical Oceanography*, *32*, 2472–2491.
- McDonald, A.M. and C. Wunsch (1996), An estimate of global ocean circulation and heat fluxes, *Nature*, *382*, 436–439.
- McPhaden, M.J. (1995), The tropical atmosphere ocean array is completed, *Bulletin of the American Meteorological Society*, *76*, 739–742.
- Niiler, P.P., N.A. Maximenko and J.C. Mc Williams (2003), Dynamically balanced absolute sea level of the global ocean, *Geophysical Research Letters*, *30*, *22*, 2164, 10.1029/2003GL018628.
- Ourmieres, Y., J.M. Brankart, L. Berline and P. Brasseur (2004), Incremental Analysis Update implementation into the intermittent data assimilation system using the SEEK filter for the ocean general circulation model OPA 8.1 in the North Atlantic $1/3^\circ$ configuration NATL3, *Mercator Technical Note*, <http://www.mercator-ocean.fr>, 38 pp.
- Özgökmen, T.M., E.P. Chassignet and C.G.H. Rooth (2001), On the connection between the

- Mediterranean outflow and the Azores Current, *Journal of Physical Oceanography*, *31*, 461–480.
- Paiva, A.M., E.P. Chassignet and A.J. Mariano (2000), Numerical simulations of the North Atlantic subtropical gyre: Sensitivity to boundary conditions and horizontal resolution, *Dynamics of Atmospheres and Oceans*, *32*, 209–238.
- Parent, L., C.E. Testut, J.M. Brankart, J. Verron, P. Brasseur and L. Gourdeau (2003), Comparative assimilation of Topex/Poseidon and ERS altimeter data and of TAO temperature data in the tropical Pacific Ocean during 1994-1998, and the mean sea-surface height issue, *Journal of Marine Systems*, *40-41*, 323–340.
- Pham, D.T., J. Verron and M.C. Roubaud (1998), Singular evolutive extended Kalman Filter with Eof initialization for data assimilation in oceanography, *Journal of Marine Systems*, *16 (3-4)*, 381–401.
- Poulain, P.M., A. Warn Varnas and P.P. Niiler (1996), Near-surface circulation of the Nordic seas as measured by Lagrangian drifters, *Journal of Geophysical Research*, *101, C8*, 18237–18258.
- Rio, M.H. and F. Hernandez (2004), A mean dynamic topography computed over the world ocean from altimetry, in situ measurements, and a geoid model, *Journal of Geophysical Research*, *109*, C12032.
- Servain, J., A.J. Busalacchi, M.J. McPhaden, A.D. Moura, G. Reverdin, M. Vianna and S.E. Zebiak (1998), A pilot research moored array in the tropical Atlantic (PIRATA), *Bulletin of the American Meteorological Society*, *79*, 2019–2031.
- Smedstad, O.M., H.E. Hurlburt, E.J. Metzger, R.C. Rhodes, J.F. Shriver, A.J. Wallcraft and

- A.B. Kara (2003), An operational eddy resolving $1/16^\circ$ global ocean nowcast/forecast system, *Journal of Marine Systems*, 40-41, 341–361.
- Smith, R.D. and M.E Maltrud (2000), Numerical simulation of the North Atlantic Ocean at $1/10^\circ$, *Journal of Physical Oceanography*, 30-7, 1532–1561.
- Stammer, D., K. Ueyoshi, A. Köhl, W.G. Large, S.A. Josey and C. Wunsch (2004), Estimating air-sea fluxes of heat, freshwater, and momentum through ocean data assimilation, *Journal of Geophysical Research*, 109 C05023, 2003JC002082.
- Sun, S., R. Bleck, C.G.H. Rooth, J. Dukowicz, E.P. Chassignet and P. Killworth (1999), Inclusion of thermobaricity in isopycnic-coordinate ocean models, *Journal of Physical Oceanography*, 29, 2719–2729.
- Treguier, A.M., S. Theetten, E.P. Chassignet, T. Penduff, R.D. Smith, L.D. Talley J.O. Beismann and C. Böning (2005), The North Atlantic Subpolar Gyre in Four High-Resolution Models, *Journal of Physical Oceanography*, 35, 757–774.

L. Parent, Sverdrup Inc., Mississippi Office, 39525 e-mail: parent@nrlssc.navy.mil

Received _____

Figure 1. Mean SSH used to reference the along track altimetry data (units are in cm, contour 8 cm), based on Niiler Mean SSH (*Niiler*, [2003]). In black color, mask of SSH: coastline, shelves, northern and southern buffer zones adjacent to the boundaries, Strait of Gibraltar, suspicious area. The black line overlain depicts the Gulf Stream maximum velocity axis from the Topex altimeter (initial 2 years, September 1992 - September 1994, *Lee*, [1997]).

Figure 2. SSH component of the fourth Eof (units are in cm, contour 1.5 cm). Low resolution (a, top left), high resolution without smoothing (b, top right), high resolution with medium smoothing (c, bottom left), high resolution with large smoothing (d, bottom right).

Figure 3. Coefficient of correction applied during the assimilation step : 0 no correction, 1 total correction.

Figure 4. RMS misfit to observations during the July, 8th 1998 - August, 4th 1999 period as a function of area (see figure 9). Left panels: T/P along track data (cm), right panels: MODAS SST data ($^{\circ}\text{C}$). The bold black curve represents the reference experiment, the bold red curve the assimilation experiment (7-day forecasts and analysis states). Along the vertical axis, the black and red crosses represent the estimation of the bias of the reference and assimilation experiments respectively. The magenta curve depicts the RMS misfit when the assimilation is turned off during the last 2 months. Left panels : the dashed black curve and the blue curve represent the RMS misfit of the reference and assimilation experiments respectively to the MODAS altimetry gridded data.

Figure 5. RMS misfit between the T/P along track data and the MODAS altimetry gridded data (units are in cm) along the fixed T/P along track positions for the Atlantic model domain and the Gulf Stream area. Time period : January 1998 - December 1999.

Figure 6. Mean SSH correction (left panel, in cm, contour 0.1cm) and mean SST correction (right panel, in °C, contour 0.1°C) during the August, 5th 1998 - August, 4th 1999 period.

Figure 7. Top: bias between the model SST from the reference simulation and the MODAS SST data during the August, 5th 1998 - August, 4th 1999 period (units are in °C, contour 0.5°C). Bottom: the same but for the assimilation experiment (7-day forecast).

Figure 8. Standard Deviation of the SSH signal during the August, 5th 1998 - August, 4th 1999 period (units are in cm, contour 4 cm, 364 daily archive files). From top to bottom, the MODAS SSH observations, the reference model experiment and the assimilation experiment (daily forecast). The black lines overlain represent the maximum velocity axis of the Gulf Stream, standard deviation and extreme positions determined from the Topex altimeter (initial 2 years, September 1992 - September 1994, *Lee, [1997]*). Blue lines show the topographic contours at 2000 and 4000 m (for longitude ≥ -63 and latitude ≥ 30).

Figure 9. Horizontal distribution of MEDS in-situ profiles, during the August, 5th 1998 - August, 4th 1999 period. The total number is the number of MEDS profiles available throughout this time period and over the entire model domain. Only profiles with depths ≥ 500 meters are used.

Figure 10. Top: temperature RMS misfit ($^{\circ}\text{C}$) with respect to the annual mean GDEM3 climatology (potential temperature) down to 750 m depth, averaged over the August, 5th 1998 - August, 4th 1999 period as a function of area. The solid curve shows the RMS misfit for the annual mean of the reference experiment and the dashed curve for the annual mean of the assimilation experiment. Along the vertical axis, the depth of the fixed positions used to estimate the RMS misfit are marked by plus signs. Bottom: temperature RMS misfit ($^{\circ}\text{C}$) with respect to MEDS profiles during the August, 5th 1998 - August, 4th 1999 period (in-situ temperature). The solid curve shows results for the reference experiment and the dashed curve for the assimilation experiment. Note that it is not the same spatial / time distribution. For the GDEM3 data it is a annual mean climatology and any profile with depths ≥ 500 meters is used. For the MEDS data, the spatial distribution is displayed on figure 9.

Figure 11. Mean surface currents of the reference experiment (top) and the assimilation experiment (bottom) during the August, 5th 1998 - August, 4th 1999 period (units are in m/s). From left to right, the southwest area of the domain and the northeast area of the domain. Blue lines show topographic contours at 2000 and 4000 m in the northeast area. Approximative position of the Flemish Cap: 44°W - 47°N . Note the speed colorbar limits are not the same in the southwest and the northeast regions. The data have been horizontally smoothed (1° , zonal component, meridional component and speed) prior to plotting. Vectors are plotted on a 1° grid and only if the speed is ≥ 0.06 m/s.

Figure 12. Mean barotropic streamfunction from the reference experiment (left) and the assimilation experiment (right) during the August, 5th 1998 - August, 4th 1999 period (units are in $10^6\text{m}^3\text{s}^{-1}$ or Sverdrup, contour 8 Sv).

Figure 13. Mean meridional overturning circulation from the reference experiment (top) and the assimilation experiment (bottom) during the August, 5th 1998 - August, 4th 1999 period (zonally averaged, units are in Sverdrup, contour 3 Sv). The white line represents the depth of the maximum MOC vs. latitude.

Figure 14. Mean meridional heat transport of the reference experiment (thin black curve, 10 archive files) and the assimilation experiment (thin red curve, 53 archive files) during the August, 5th 1998 - August, 4th 1999 period (units are in PW). The bold dashed red curves represent the mean \pm one standard deviation of the assimilation experiment when each weekly snapshot is smoothed with a 6° latitude window. Vertical blue lines represent values and error bars estimated by *Ganachaud and Wunsch*, [2003] (solid line) and *McDonald and Wunsch*, [1996] (dashed line). The tropical band ($\pm 15^\circ$) is represented by the bold black line.

Figure 15. Top: mean mixed layer depth of the reference experiment (left) and the assimilation experiment (right) during the March 3rd 1999 - March 31th 1999 period (units are in meters, contour 200 m). Black lines show the topographic contour at 2000 m. The position of the bravo station is located at 51.5°W - 56.5°N (+ symbol). Approximative position of the Cape Farewell and the Cape Desolation are represented by the black spots. Bottom: bias between the model SSS from the reference experiment (left) or the assimilation experiment (right) and the SSS GDEM3 data during the August, 5th 1998 - August, 4th 1999 period (units are in psu, contour 0.15 psu).

Figure 16. RMS misfit to GDEM3 SSS in the Labrador and Irminger areas (units are in psu). The solid curve represents the reference experiment and the dashed curve the assimilation experiment (7-day forecasts and analysis states).

Figure 17. Salinity RMS misfit (psu) with respect to the annual mean GDEM3 climatology down to 750 m depth, averaged over the August, 5th 1998 - August, 4th 1999 period as a function of area. The solid curve shows the RMS misfit for the annual mean of the reference experiment and the dashed curve for the annual mean of the assimilation experiment. Along the vertical axis, the depths of the fixed positions used to estimate the RMS misfit are marked by plus signs. Only profiles with depths ≥ 500 meters are used.

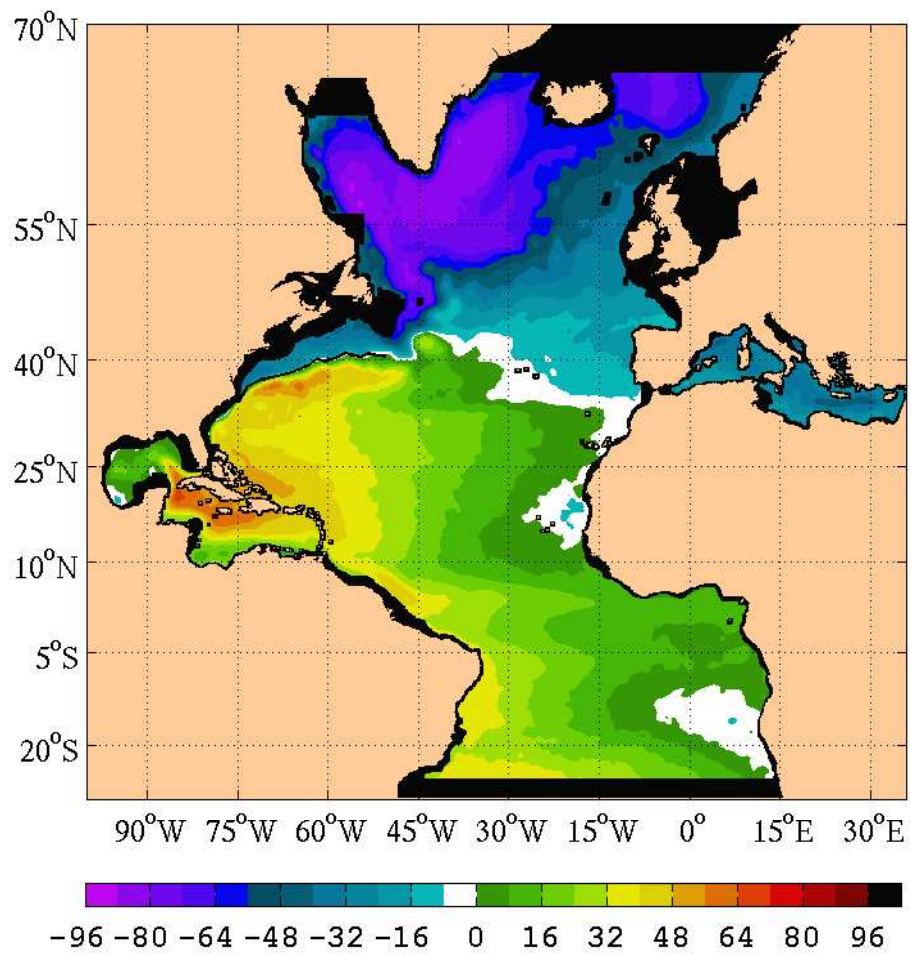


Figure 1

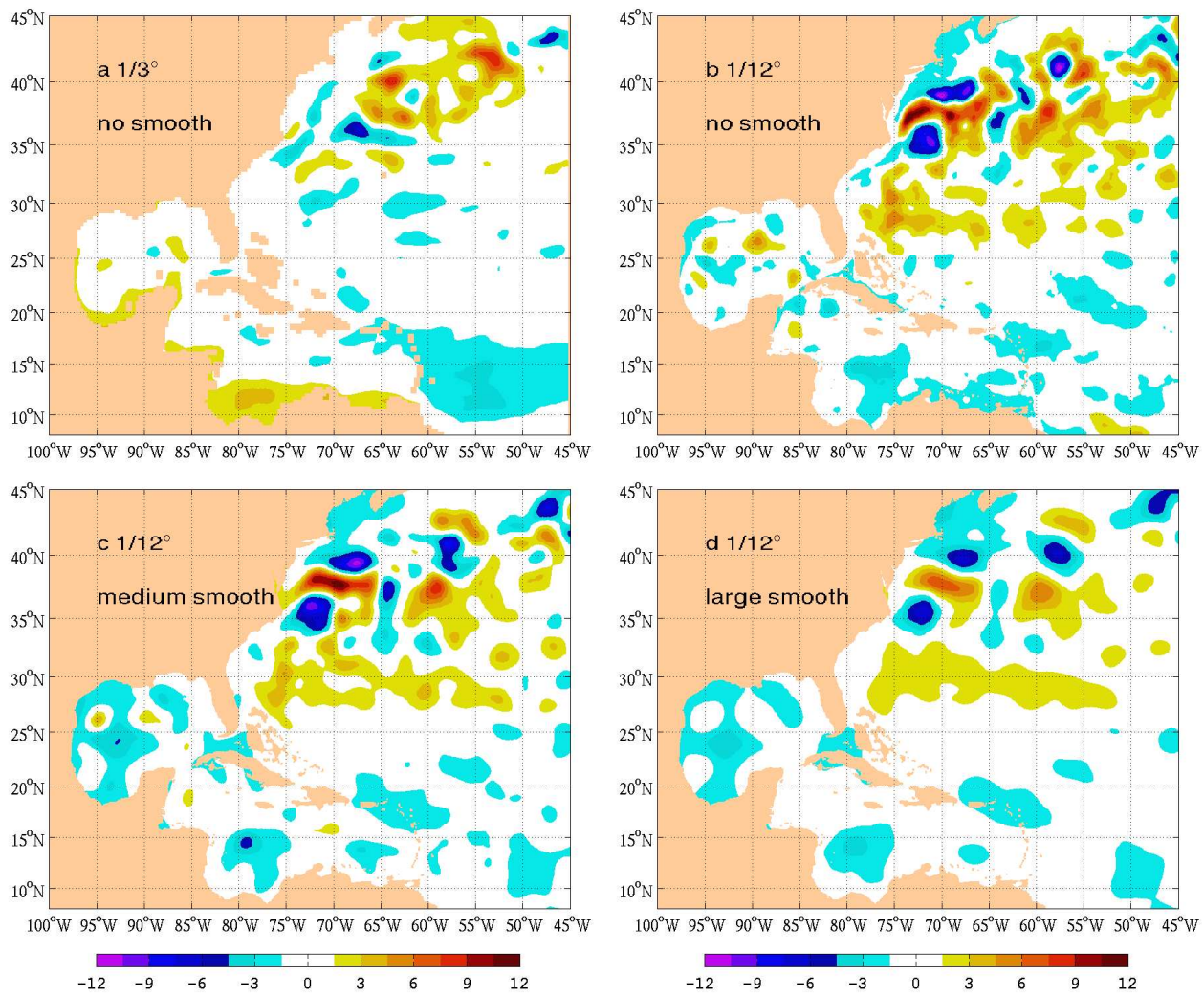


Figure 2

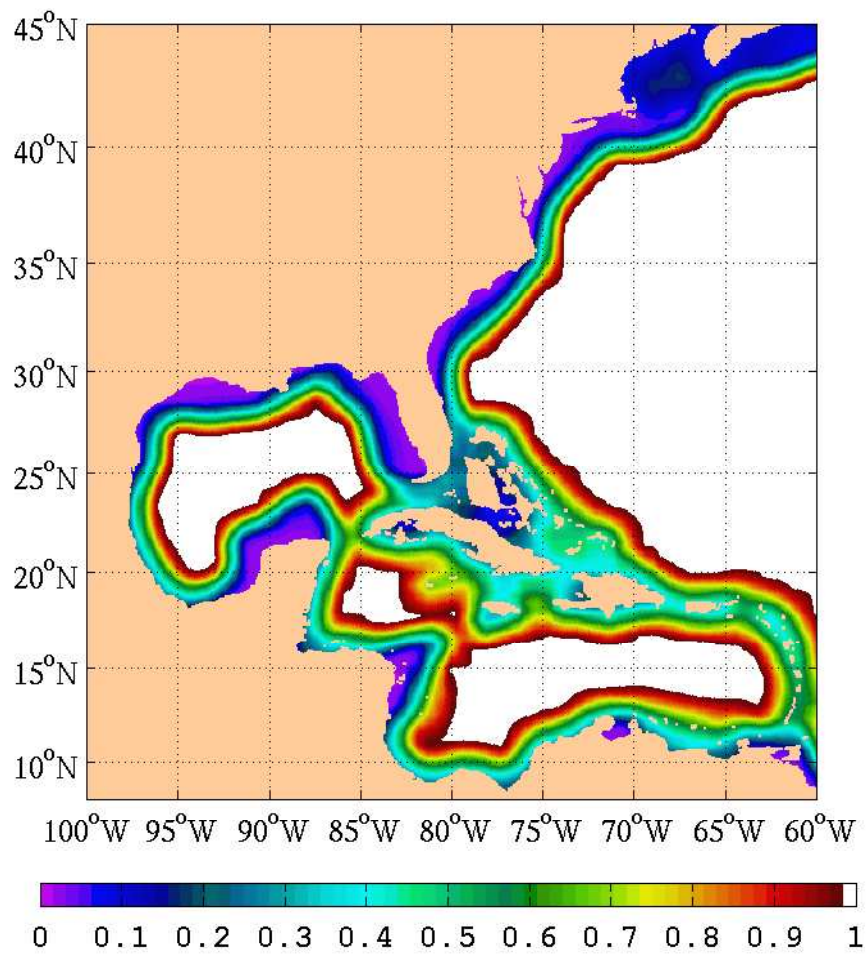


Figure 3

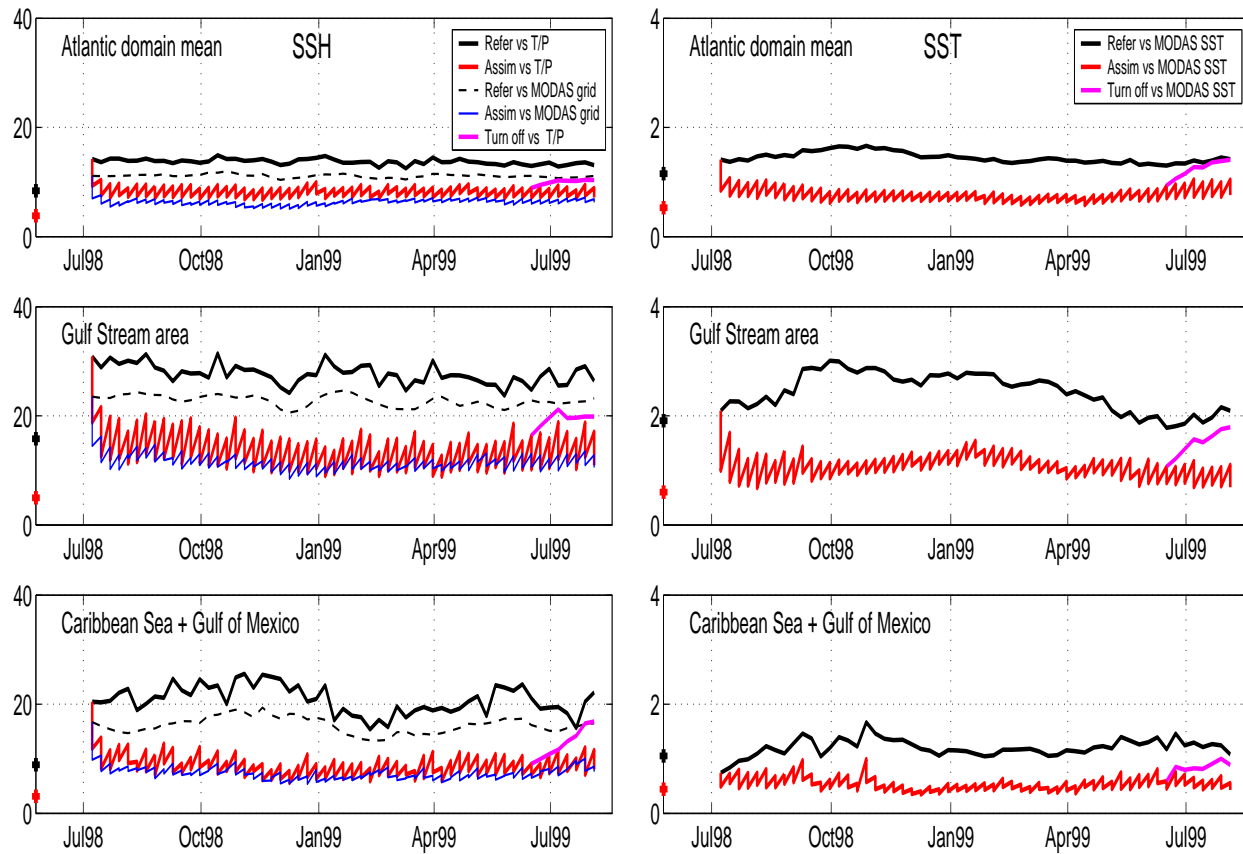


Figure 4

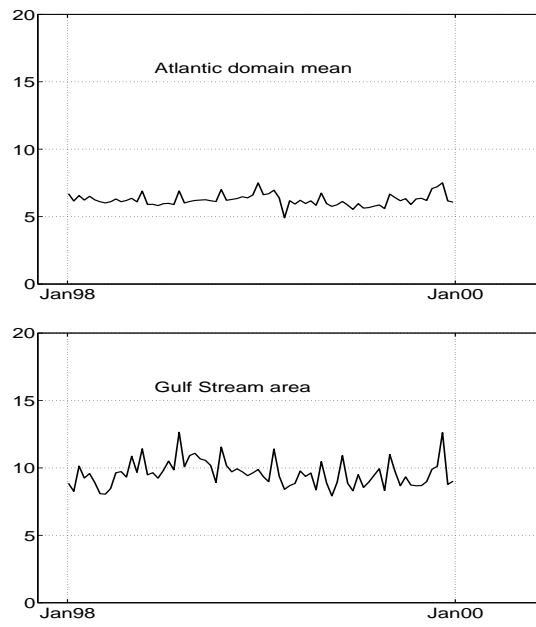


Figure 5

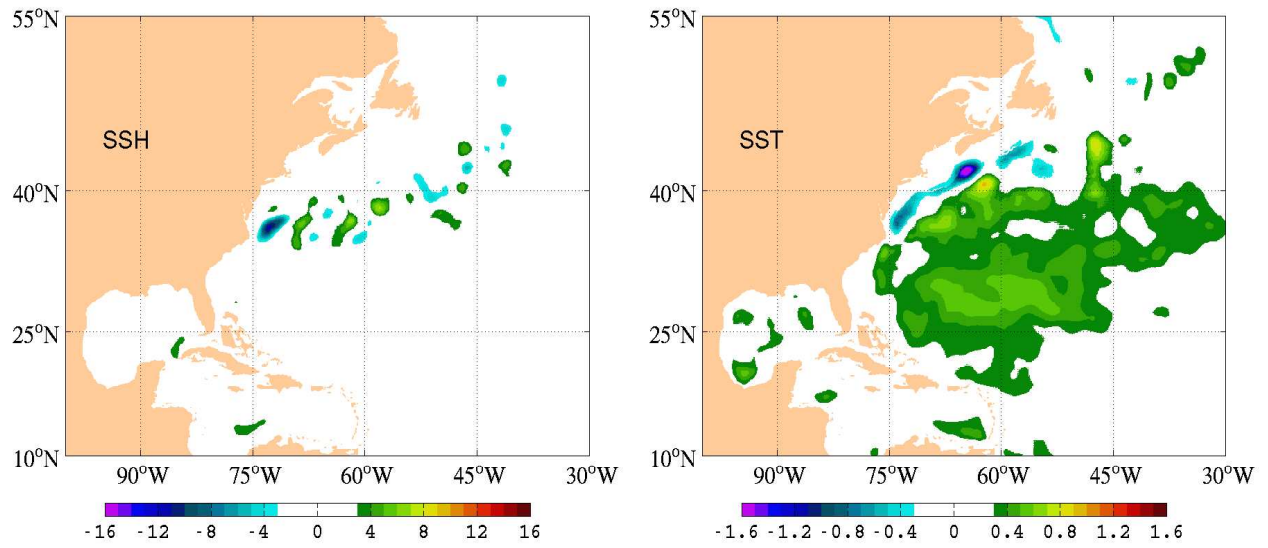


Figure 6

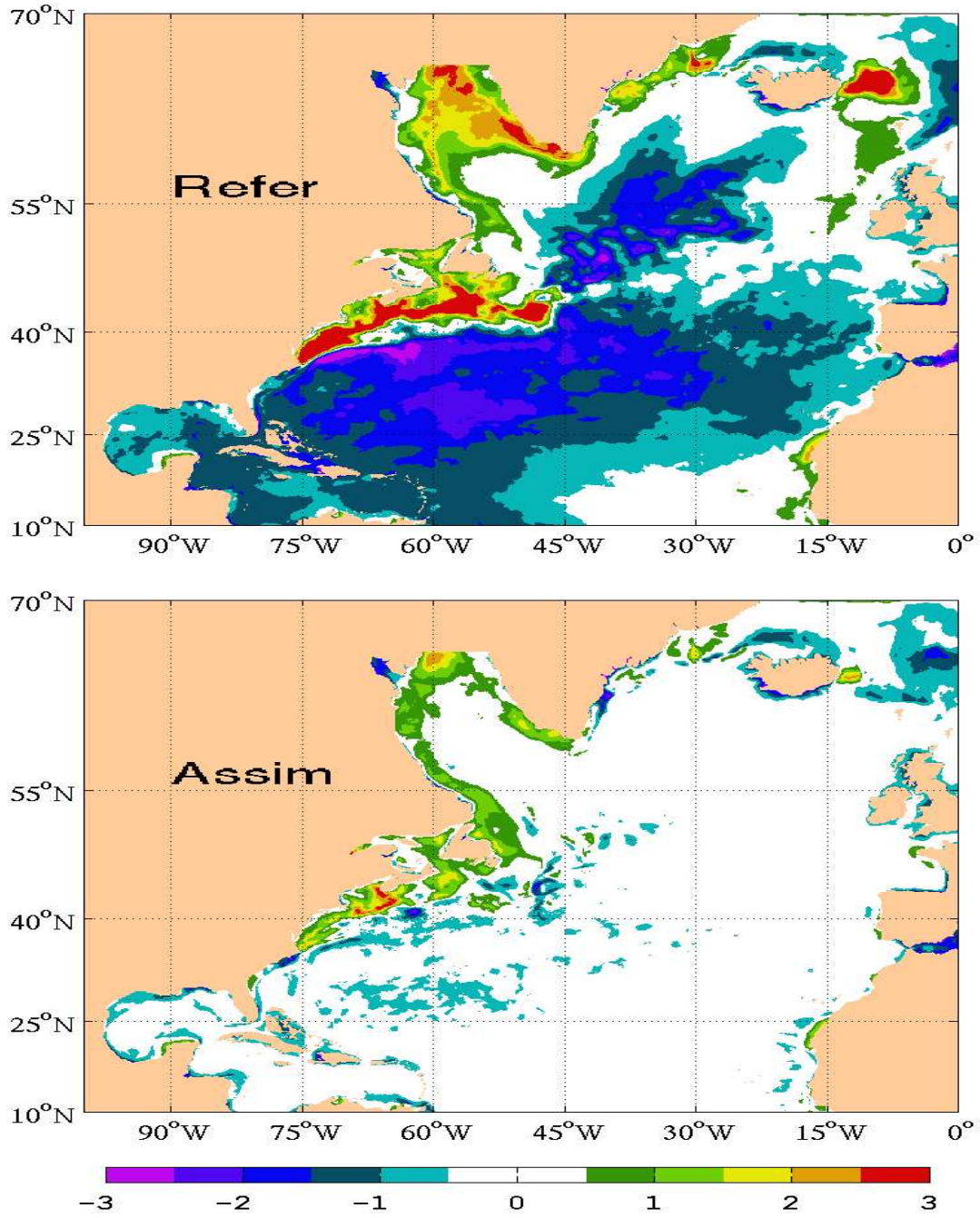


Figure 7

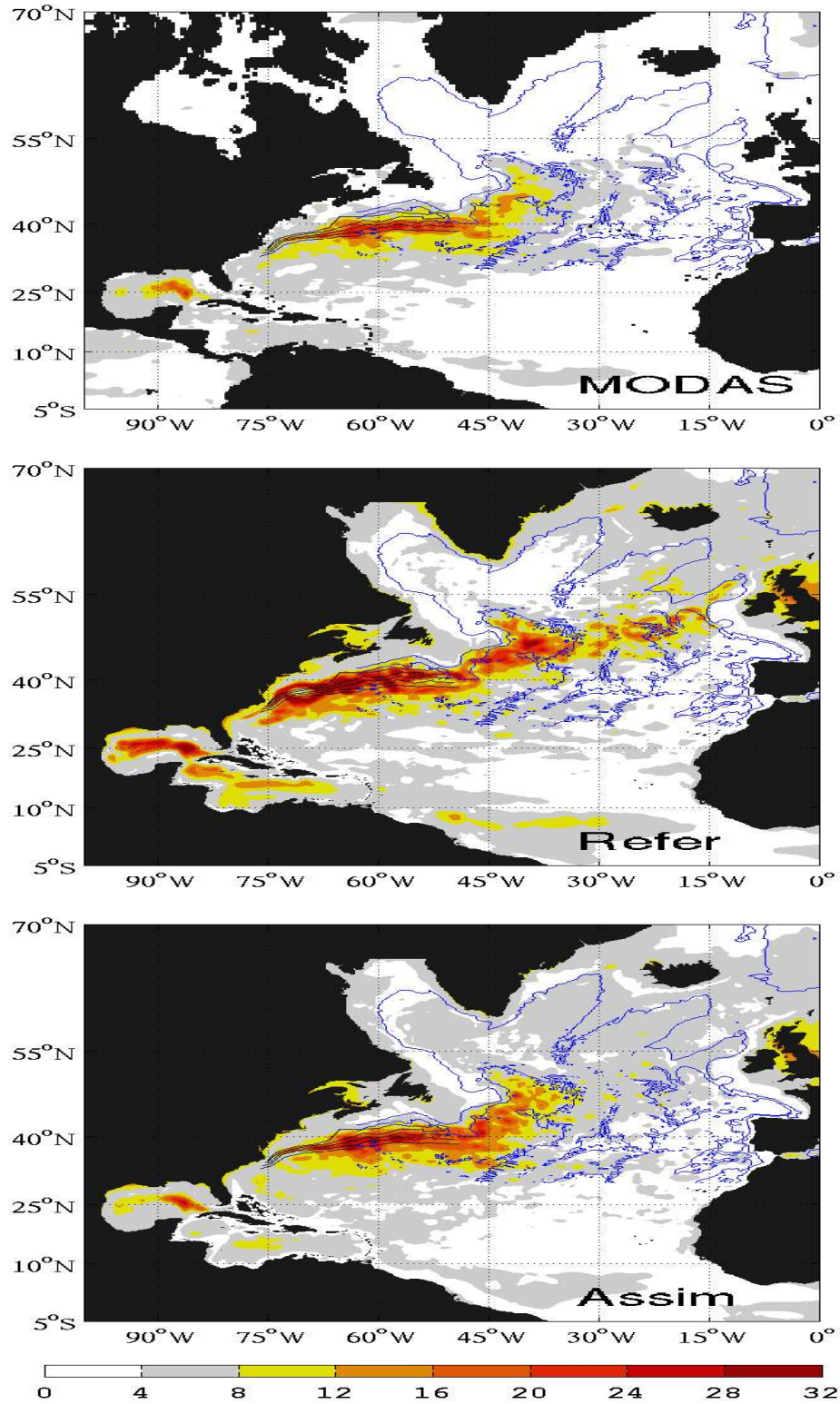


Figure 8

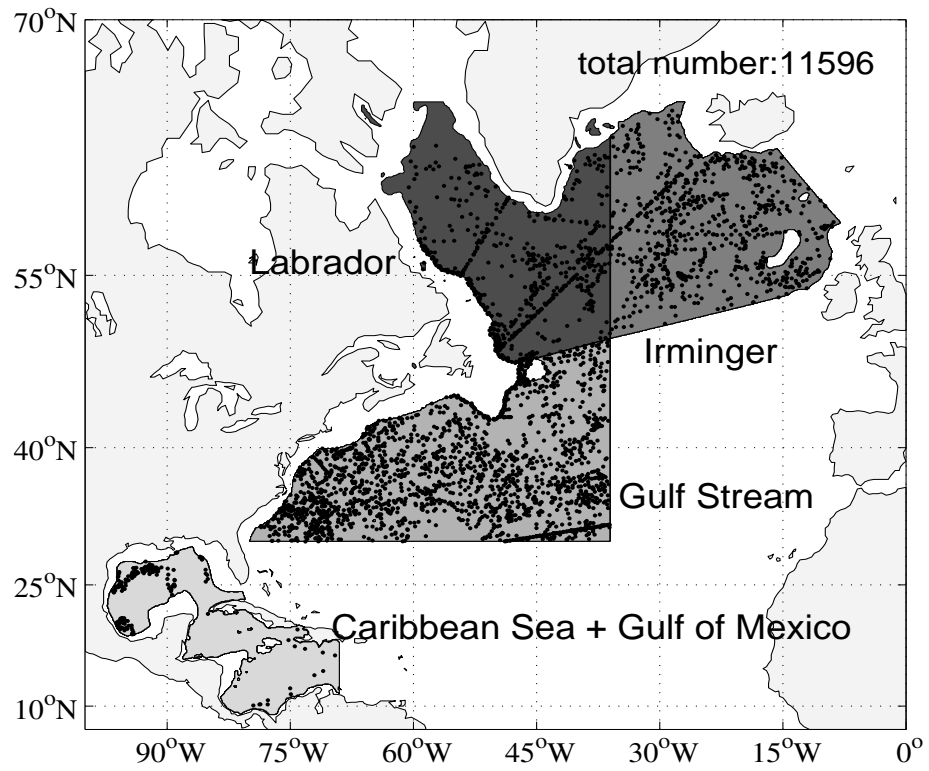


Figure 9

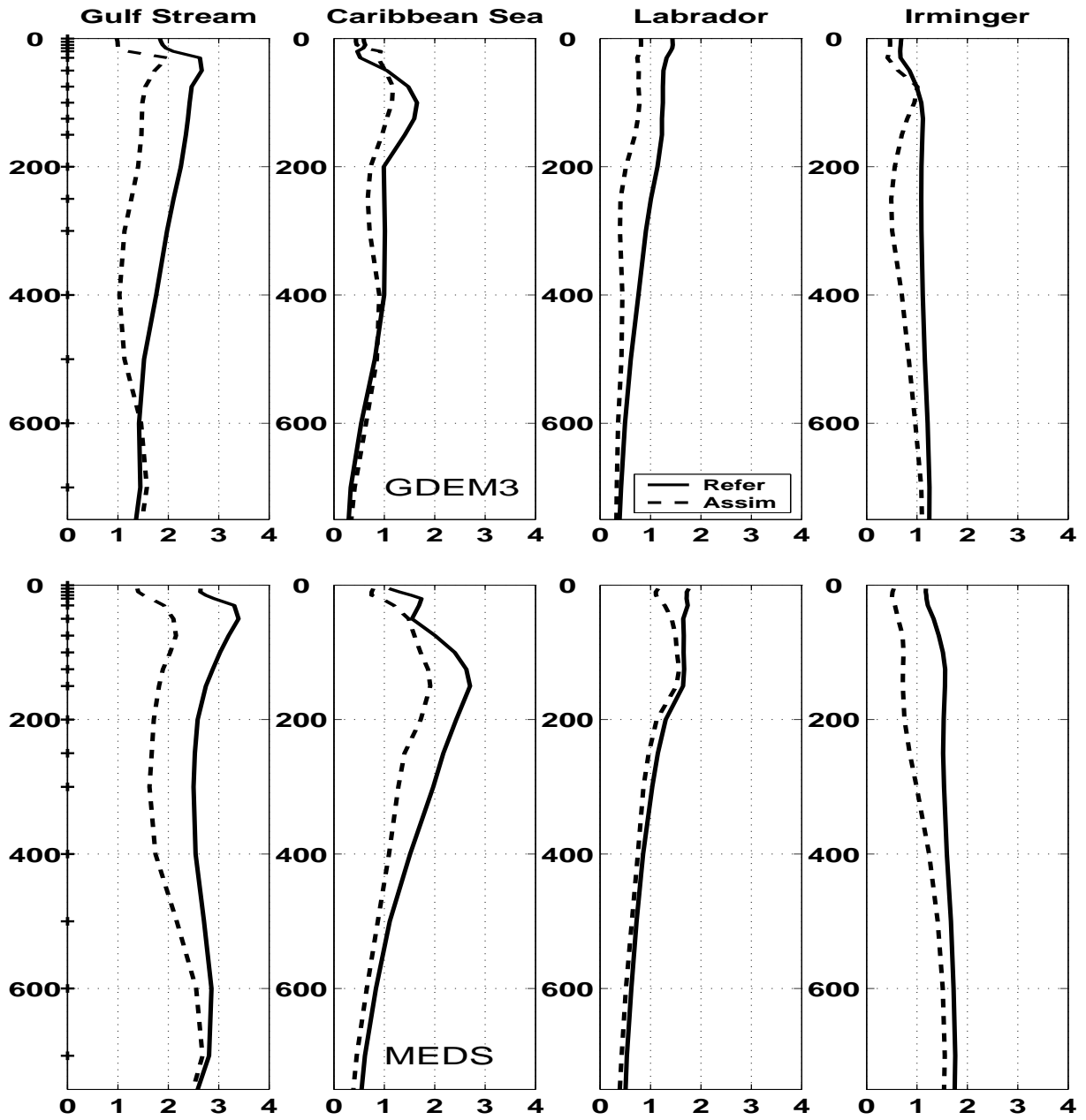


Figure 10

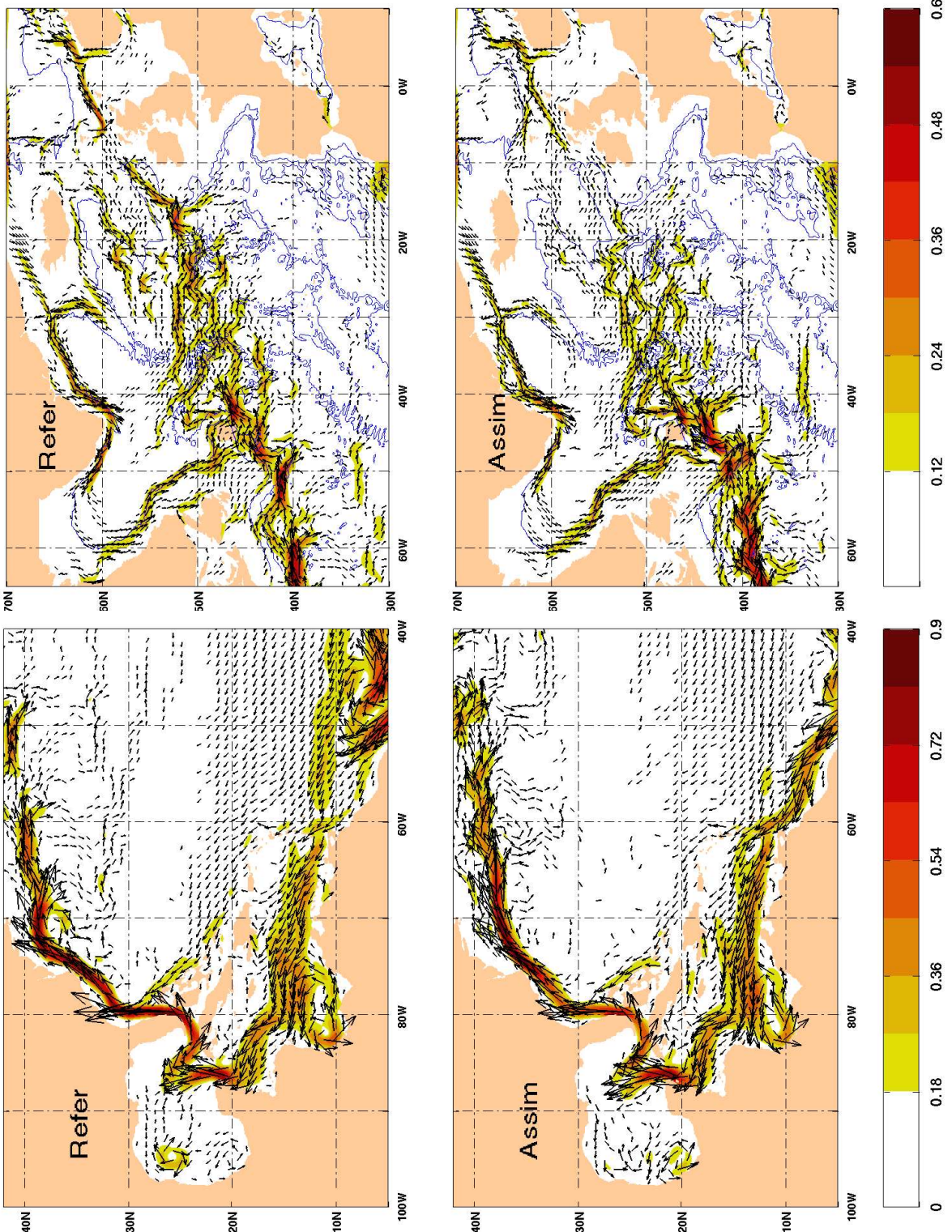


Figure 11

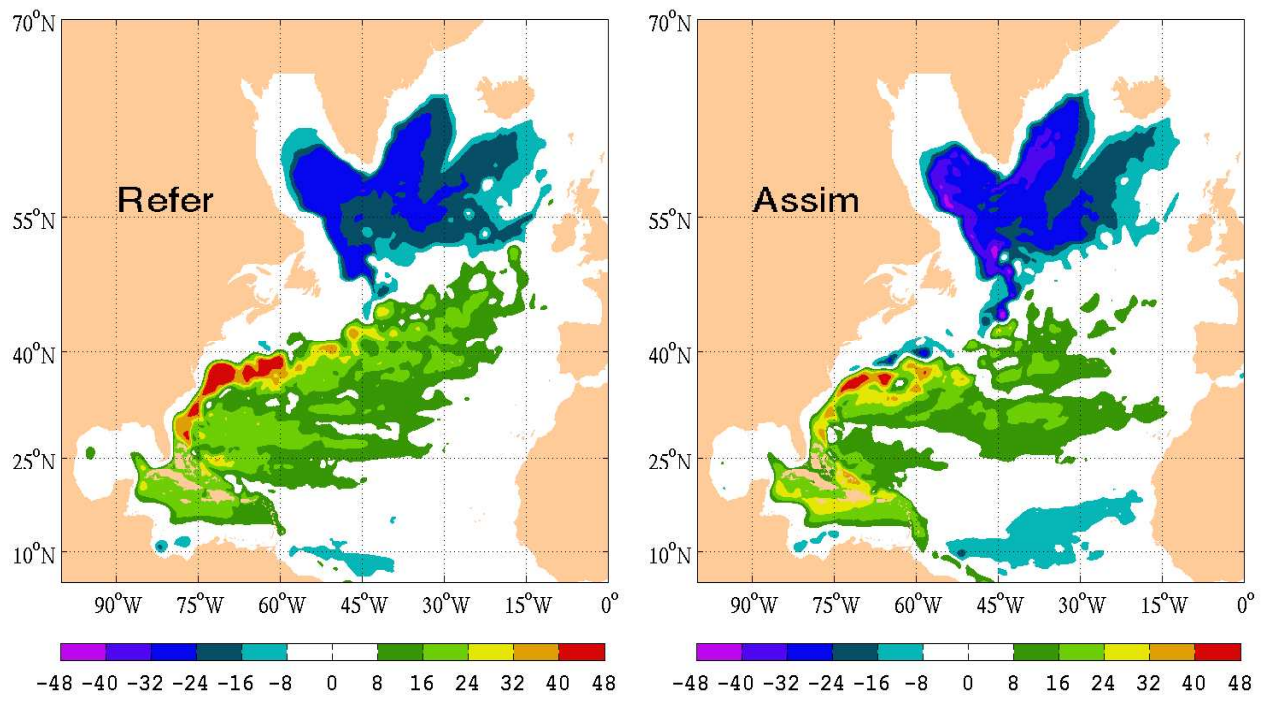


Figure 12

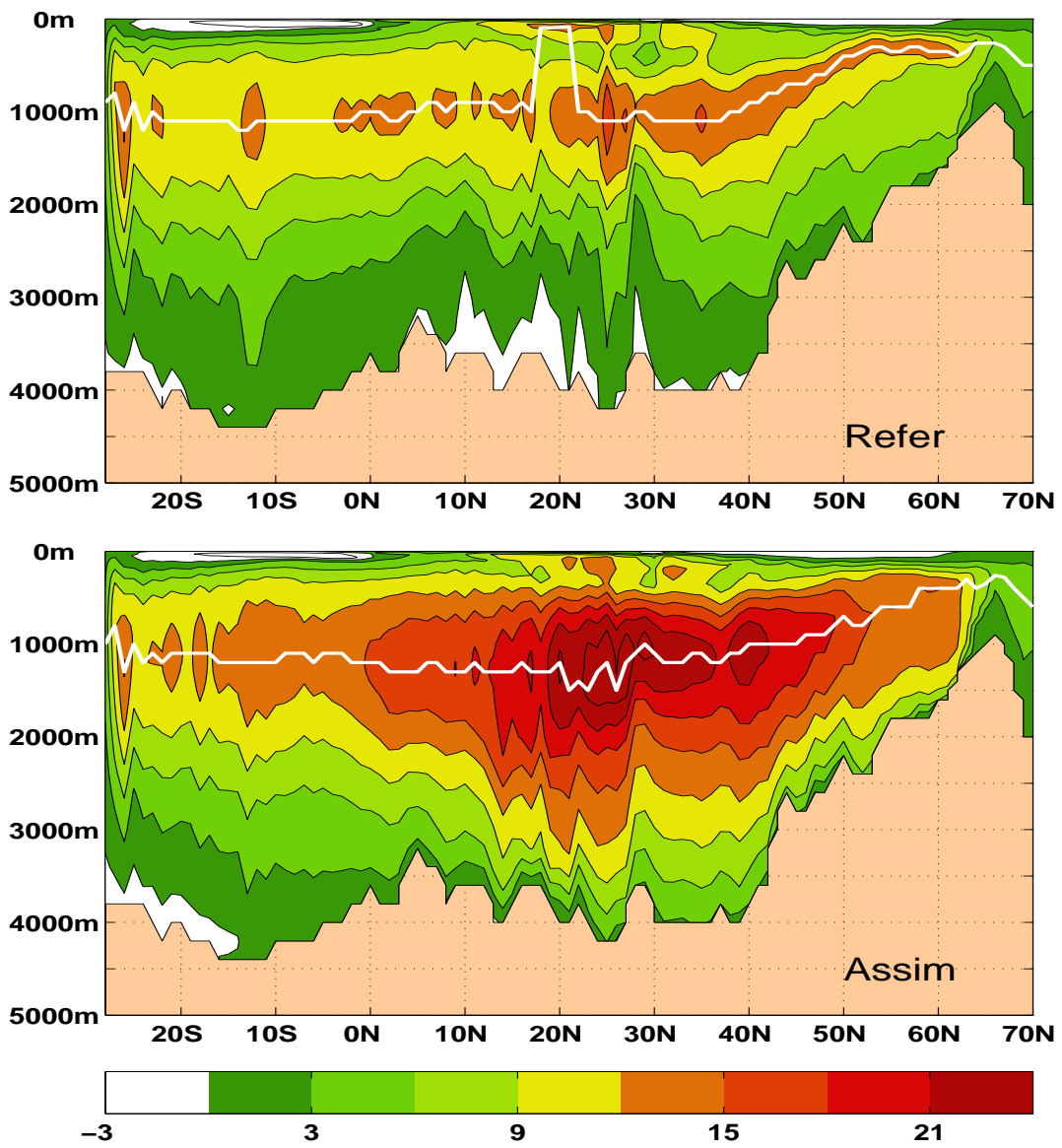


Figure 13

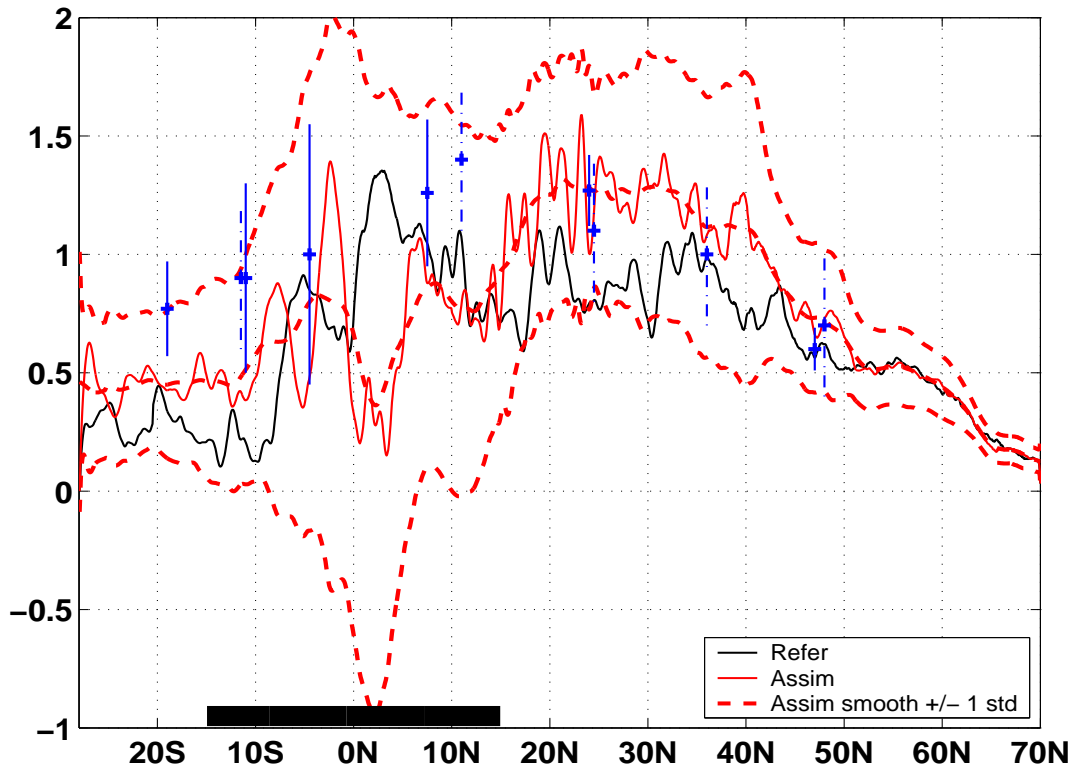


Figure 14

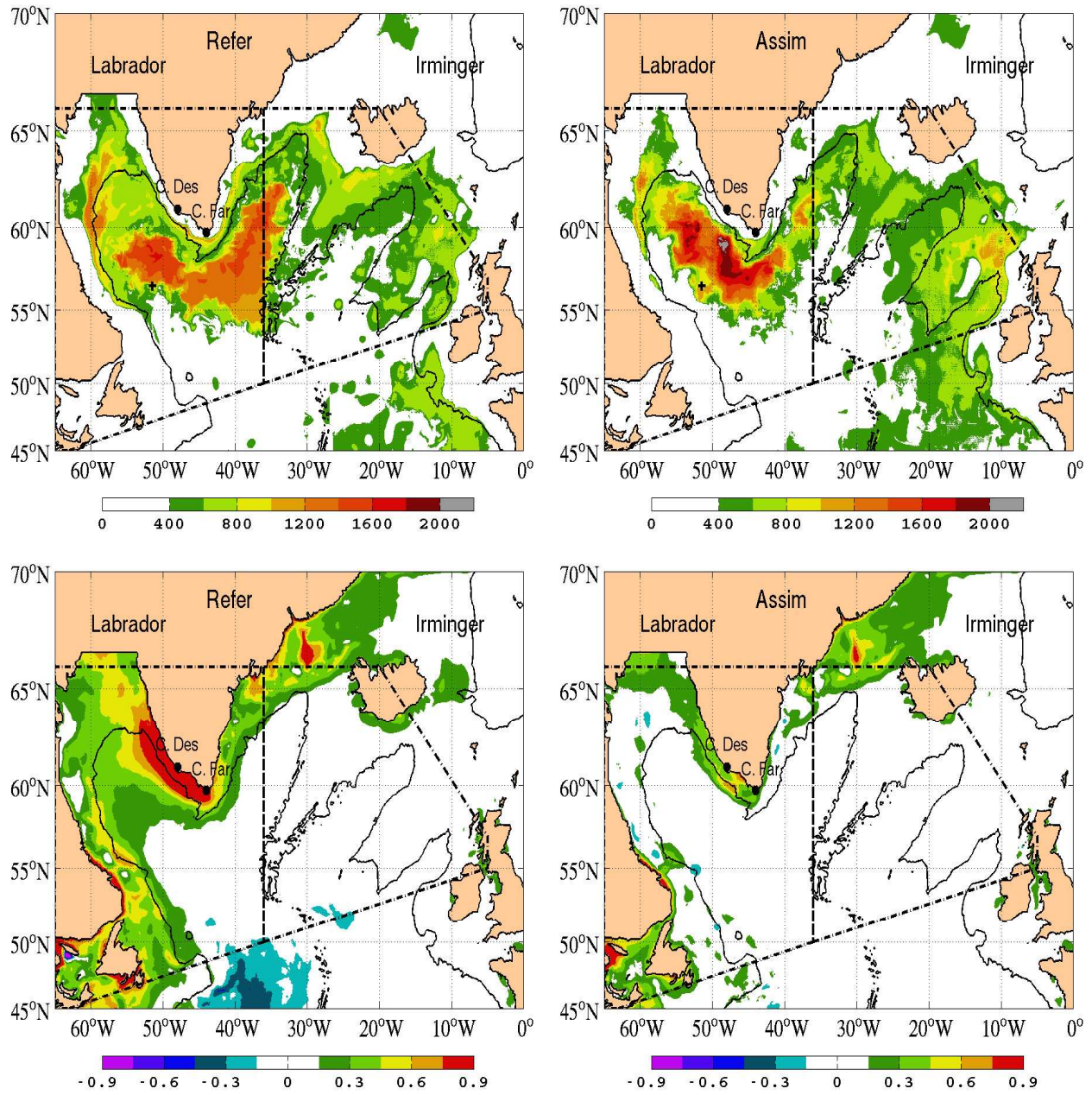


Figure 15

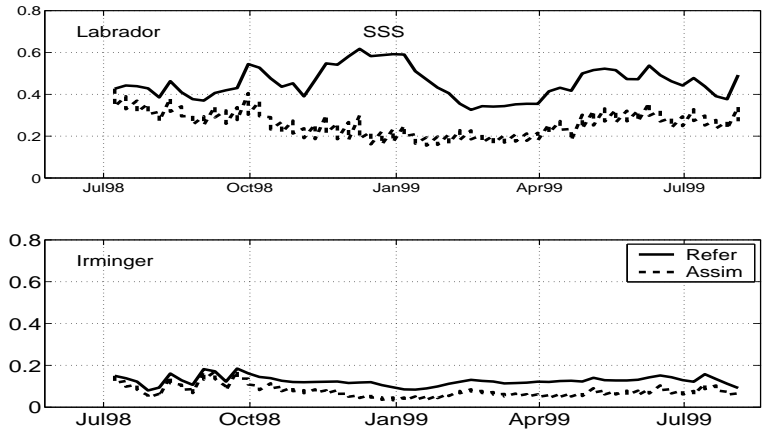


Figure 16

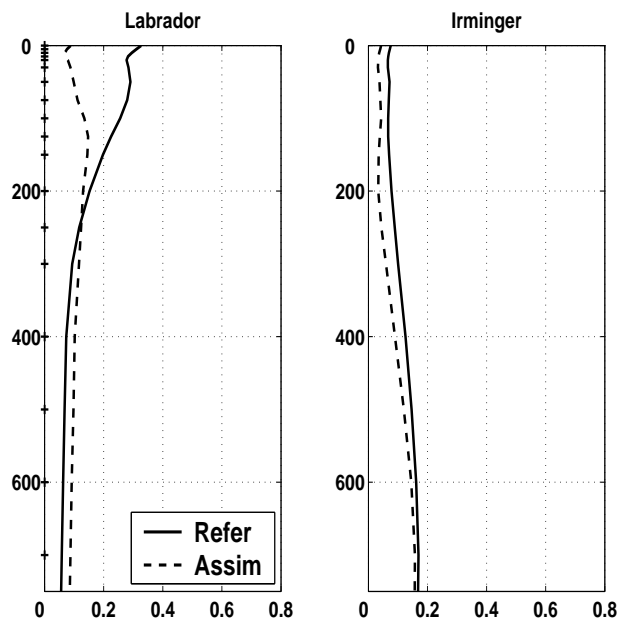


Figure 17